European Reviews of Chemical Research

Has been issued since 2014. ISSN 2312-7708, E-ISSN 2413-7243
2015. Vol.(5). Is. 3. Issued 4 times a year

The journal is registered by Federal Service for Supervision of Mass Media, Communications and Protection of Cultural Heritage (Russian Federation). Registration Certificate **ПИ № ФС77-57042** 25.02.2014.

Journal is indexed by: **CrossRef** (UK), **Electronic scientific library** (Russia), **Journal Index** (USA), **Open Academic Journals Index** (Russia), **ResearchBib** (Japan), **Scientific Indexing Services** (USA)

All manuscripts are peer reviewed by experts in the respective field. Authors of the manuscripts bear responsibility for their content, credibility and reliability.

Editorial board doesn't expect the manuscripts' authors to always agree with its opinion.

Postal Address: 26/2 Konstitutcii, Office 6
354000 Sochi, Russian Federation

Website: http://ejournal14.com/en/index.html
E-mail: evr2010@rambler.ru
Founder and Editor: Academic Publishing House *Researcher*

Passed for printing 15.09.15.
Format 21 × 29,7/4.
Enamel-paper. Print screen.
Headset Georgia.
Ych. Izd. l. 5,1. Ysl. pech. l. 5,8.
Circulation 500 copies. Order № 105.

European Reviews of Chemical Research

2015

Is. 3

Европейские обзоры химических исследований

2015

№ 3

Европейские обзоры химических исследований

Издается с 2014 г. ISSN 2312-7708, E-ISSN 2413-7243
2015. № 3 (5). Выходит 4 раза в год.

Журнал зарегистрирован Федеральной службой по надзору в сфере массовых коммуникаций, связи и охраны культурного наследия (Российская Федерация). Свидетельство о регистрации средства массовой информации **ПИ № ФС77-57042** 25.02.2014.

Журнал индексируется в: **CrossRef** (Великобритания), **Journal Index** (США), **Научная электронная библиотека** (Россия), **Open Academic Journals Index** (Россия), **ResearchBib** (Япония), **Scientific Indexing Services** (США)

Статьи, поступившие в редакцию, рецензируются. За достоверность сведений, изложенных в статьях, ответственность несут авторы публикаций.
Мнение редакции может не совпадать с мнением авторов материалов.

Адрес редакции: 354000, Российская Федерация, г. Сочи, ул. Конституции, д. 26/2, оф. 6
Сайт журнала: **http://ejournal14.com**
E-mail: **evr2010@rambler.ru**

Учредитель и издатель: ООО «Научный издательский дом "Исследователь"» - Academic Publishing House *Researcher*

Подписано в печать 15.09.15.
Формат 21 × 29,7/4.
Бумага офсетная.
Печать трафаретная.
Гарнитура Georgia.
Уч.-изд. л. 5,1. Усл. печ. л. 5,8.
Тираж 500 экз. Заказ № 105.

C O N T E N T S

Published in the Russian Federation
European Reviews of Chemical Research
Has been issued since 2014.
ISSN: 2312-7708
E-ISSN: 2413-7243
Vol. 5, Is. 3, pp. 144-165, 2015

DOI: 10.13187/ercr.2015.5.144
www.ejournal14.com

UDC 579.871.08:577.112.385.4.08

The Development of Biosynthesis of 2H- and 13C-labeled Amino acids and Proteins with Various Levels of Isotopic Enrichment Using Bacterial Objects

[1]*Oleg Mosin
[2] Ignat Ignatov
[3] Dmitry Skladnev
[4] Vitaly Shvets

[1] Moscow State University of Applied Biotechnology, Russian Federation
Senior research Fellow of Biotechnology Department, Ph. D. (Chemistry)
103316, Moscow, Talalihina ulitza, 33
*E-mail: mosin-oleg@yandex.ru
[2] The Scientific Research Center of Medical Biophysics (SRC MB), Bulgaria
Professor, D. Sc., director of SRC MB
1111, Sofia, N. Kopernik street, 32
E-mail: mbioph@dir.bg
[3] Scientific Center of Russian Federation Research Institute for Genetics and Selection of Industrial Microorganisms “Genetika”, Russian Federation
Professor, D. Sc (Biology), leading scientist of “Genetika”
117545, Moscow, 1st Dorozhniy proezd, 1
E-mail: genetika@genetika.ru
[4] M.V. Lomonosov Moscow University of Fine Chemical Technology, Russian Federation
Academician of Russian Academy of Sciences, D. Sc. (Chemistry), head of the department of biotechnology and nanobiotechnology
119571, Moscow, Vernadskogo avenue, 86
E-mail: mitht@mitht.ru

Abstract

By the method of microbiological synthesis were obtained and analyzed by electron impact mass-spectrometry 2H, 13C-labeled amino acids of a facultative methylotrophic bacterium Brevibacterium methylicum and an obligate methylotrophic bacterium Methylobacillus flagellatum and 2H, 13C-labeled amino acids of the total protein of biomass obtained on media containing as a source of stable isotopes [2H]methanol, [13C]methanol and 2H2O. It was also performed the incorporation of L-[2,3,4,5,6-2H]phenylalanine, L-[3,5-2H]tyrosine and L-[2,4,5,6,7-2H]tryptopan into the membrane integral protein bacteriorhodopsin synthesised in purple membranes of photo-organotrophic halobacterium Halobacterium halobium ET 1001. For mass-spectrometric analysis the multicomponential mixtures of 2H- and 13C-labeled amino acids, derived from cultural media and protein hydrolysates after hydrolysis in 6 M 2HCl (3% phenol) and 2 M Ba(OH)2 were modified into N-benzyloxycarbonyl-derivatives of amino acids as well as into methyl esters of N-5-(dimethylamino)naphthalene-1-sulfonyl chloride (dansyl) derivatives of [2H, 13C]amino acids,

which were preparative separated using a method of reverse-phase HCLP. Biosynthetically obtained 2H- and 13C-labeled amino acids represented the mixtures differing in quantities of isotopes incorporated into molecule. The levels of 2H and 13C enrichment of secreted amino acids and amino acid resigues of protein were found to vary from 20,0 atom.% to L-leucine/isoleucine up to 97,5 atom.% for L-alanine depending on concentration of 2H- and 13C-labelled substrates.

Keywords: stable isotopes, methylotrophic bacteria, halobacteria, isotope labeled amino acids, bacteriorhodopsin

Introduction

The enrichment of molecules by stable isotopes (2H, 13C, 15N, 18O) is an important tool for a variety of biochemical and metabolic studies with amino acids and other biologically active substances (BAS) [1]. The preferential usage of stable isotopes as compared to their counterparts are stipulated by the lack of radioactive radiation hazards and determination of the localization of the label in the molecule by high resolution techniques, including NMR [2], IR spectroscopy [3], and mass spectrometry [4]. The development of these methods for the detection of stable isotopes in biological probes in recent years has significantly increased the efficiency of biological research, as well as studies of the structure and mechanism of action of cellular BAS at the molecular level. In particular, 2H- and 13C-labeled amino acids are used for studying of the spatial structure and conformational changes of proteins, the interaction of protein molecules and in chemical syntheses of some isotope-labeled compounds based on them [5]. For example, isotopically labeled L-phenylalanine is used in the synthesis of peptide hormones and neurotransmitters [6].

An important factor in studies using labeled amino acids is their accessibility. 2H and 13C-labeled amino acids can be prepared using chemical, enzymatic and microbiological methods. The chemical synthesis is multistage often requires a large expenditure of costly labeled reagents and substrates and leads to a racemic mixture of D- and L-enantiomers for separation of which is required the special separation methods [7]. Fine chemical synthesis of 2H- and 13C-labeled amino acids is linked with using a combination of chemical and enzymatic approaches [8].

Microbiology provides an alternative to chemical synthesis a method for obtaining 2H- and 13C-labeled amino acids, which leads to high yields of the synthesized products, the effective incorporation of stable isotopes in the molecule, and preservation of the natural configuration of synthesized [2H, 13C] compounds. For the preparation of biosynthetic 2H- and 13C-labeled amino acids use several approaches, one of which is consisted in uniform enrichment of synthesized compounds at the carbon skeleton in the molecule due to using the bacterial strains growing on selective media containing as a source of stable isotopes [13C] methanol, [2H]methanol and 2H2O [9, 10]. This approach also involves the use of complex chemical components of biomass grown on [2H, 13C] growth substrates with further separating and fractionating of target 2H- and 13C-labeled compounds. Another approach is a site-specific enrichment of amino acids at certain positions of molecules due to assimilation by cell the isotopically labeled precursors such as [1,4-13C]succinate, [1, 2-13C]acetate and [1-13C]lactate [11].

The present work is a continuation of the research toward to the biosynthetic preparation of 2H- and 13C-labeled amino acids due to the disposal by the cell of low-molecular labeled substrates – [2H]methanol, [13C]methanol and 2H2O followed by the monitoring of the inclusion of stable isotopes of 2H and 13C into molecules of biosynthesized amino acids by electron impact mass spectrometry. The sensitivity of EI mass spectrometry is 10-9–10-11 mol in samples, which is considerably higher than the IR and NMR spectroscopy. This method combined with RP-HPLC method has worked well for the study of the level of isotopic enrichment of [2H, 13C]amino acid molecules in the composition of their multi component mixtures as the samples of culture liquids of bacterial strains, producers of amino acids and hydrolysates of total protein of biomass obtained on the minimal growth medium M9 containing isotopic labeled substrates.

Material and methods

Objects of research

Investigations were carried out with genetically marked strains of bacteria obtained from the culture collection of the Russian National Collection of Industrial Microorganisms (PMBC) State Research Institute of Genetics and Selection of Industrial Microorganisms:

1) Brevibacterium methylicum VKPM B 5652 – L-leucine-dependent strain of facultative methylotrophic bacteria producing L-phenylalanine;

2) Methylobacillus flagellatum KT – L-isoleucine-dependent strain of obligate methylotrophic bacteria producing L-leucine;

3) Halobacterium halobium ET 1001 – the pigment-containing strain of photo organotrophic halobacteria, the ability to synthesize bacteriorhodopsin.

Chemicals

In the research was used 2H2O (99,9 atom.% 2H), 2HCl (95,6 atom.% 2H), [2H]methanol (98,5 atom.% 2H) and [13C]methanol (99,5 atom.% 13C) obtained from the Russian Scientific-technical Center "Isotope" (St. Petersburg, Russia). L-[2,3,4,5,6-2H5]phenylalanine (90 atom.% 2H), L- [3,5-2H2]tyrosine (96 atom.% 2H) and L-[2,4,5,6,7-2H5]tryptophan (98 atom.% 2H) were obtained by chemical isotopic exchange (methods of obtaining are listed in [12]). For the synthesis of amino acids used N-5-(dimethylamino)naphthalene-1-sulfonyl chloride (dansyl chloride), chem. pur. ≥99,0% (HPLC) (Sigma Aldrich, USA), benzyloxycarbonyl (CBz-chloride), ≥98,0% (HPLC) (Sigma Aldrich, USA) and diazomethane, prepared from N-nitrosomethylurea, ≥99,0% (HPLC) (Sigma Aldrich, USA).

Growth conditions of microorganisms and isolation
of 2H, 13C-labeled proteins and amino acids

The cultivation of methylotrophic bacteria B. methylicum and M. flagellatum was performed in a mineral M9 medium in Erlenmeyer flasks with 250 ml volume filled up with 50 ml of the growth medium as described in [13], using as a source of stable isotopes [2H]methanol, [13C]methanol and 2H2O in the presence of L-leucine for B. methylicum and L-isoleucine for M. flagellatum in concentrations of 10 mg/l. Cells were separated by centrifugation in the centrifuge T-24 ("Heraues Sepatech", Germany) (10000 g, 20 min). In the culture liquids were analyzed the secreted amino acids.

To isolate the protein fraction of the total biomass the cells were washed twice with distilled water followed by centrifugation (10000 g, 20 min), exposed to ultrasound at 40 kHz (3×15 min) and centrifuged. The resulting precipitate (10 mg) obtained after the separation of lipids and pigments by a mixture of organic solvents: chloroform–methanol–acetone (2: 1: 1) was used as the protein fraction of the total biomass.

For biosynthesis of deuterium labeled bacteriorhodopsin used the synthetic medium containing 18 amino acids, wherein unlabelled aromatic L-amino acids – phenylalanine, tyrosine and tryptophan were replaced by their deuterated analogues – L-[2,3,4,5,6-2H5]phenylalanine, L-[3,5- 2H2]tyrosine and L-[2,4,5,6,7-2H5]tryptophan (the amounts of components are given in g/l): (D,L-alanine – 0,43; L-arginine – 0,4; D,L-aspartic acid – 0,45; L-cysteine – 0,05; L-glutamic acid – 1,3; L-glycine – 0,06; D,L-histidine – 0,3; D,L-isoleucine – 0,44; L-leucine – 0,8; L-lysine – 0,85; D,L-methionine – 0,37; L-phenylalanine – 0,26; L-proline – 0,05; D,L-serine – 0,61; D,L-threonine – 0,5; L-tyrosine – 0,2; D,L-tryptophan – 0,5; D,L-valine – 1,0); nucleotides (adenosine-5-monophosphate – 0,1; uridine-5-monophosphate – 0,1); salts (NaCl – 250; MgSO4.7H2O – 20, KCI – 2; NH4Cl – 0,5; KNO3 – 0,1; KH2PO4 – 0,05; K2HPO4 – 0,05; sodium citrate – 0,5; MnSO4.H2O – 3,10-4; CaCl2.6H2O – 0,065; ZnSO4.7H2O – 4,10-5; FeSO4.7H2O – 5,10-4; CuSO4.H2O – 5.10-5); glycerin – 1,0; growth factors (biotin – 0,1.10-3; folic acid – 10.10-3; vitamin B12 – 2.10-4).

For the isolation of the purple membrane the cell fraction obtained after the separation of the culture liquid and washing with doubly distilled water (100–150 mg) was suspended in 100 ml of 0,1 M Tris-HCl (pH = 7,6), then 1 mg of DNase I were added and incubated for 5–6 hours at 37 0C, then diluted with distilled water to 200 ml and incubated for 15 hours at 4 0C. The precipitate was washed with distilled water followed by separation of the aqueous fraction to give colorless washing water. The purity of the resulting purple membrane suspension (in H2O) was monitored with a spectrophotometer Beckman DU-6, (Beckman Coulter, USA) at the ratio of the absorption bands at λ = 280/568 nm (molar absorbance coefficients: ε280 = 1,1.105 M-1 cm-1 [14] and ε568 = 6,3.104 M-1 cm-1 [15]).

Bacteriorhodopsin was isolated by the method of D. Osterhelta [16], improved by the authors due to the colloidal dissolution (solubilization) of bacteriorhodopsin containing purple membrane fraction (50 mg) in 2 ml of 0,5% of sodium dodecyl sulfate (SDS) in H2O and precipitating protein by 5 fold excess of methanol in the cold (0 0C). The imput of bacteriorhodopsin was 17–20 mg.

Pigments and lipids extracted with chloroform–methanol–acetone (2: 1: 1) according to Bligh and Dyer method [17].

Hydrolysis of total protein was performed with 6 M 2HCl (3% phenol in 2H2O) or 2 M Ba(OH)2 (+110 0C, 24 h).

Synthesis of N-Dns-[2H, 13C] amino acids

For the synthesis of N-Dns-[2H, 13C]amino acids to 4–5 mg of lyophilized samples of culture liquid and protein hydrolysates dissolved in 1 ml of 2 M NaHCO3, pH = 9–10 was added portionwise with stirring 25,5 mg of dansyl chloride in 2 ml of acetone. The reaction mixture was kept under stirring for 1 hour at t = 40 0C, then acidified with 2 M HCl to pH = 3,0 and extracted with ethyl acetate (3×5 ml). The combined extract was washed with water until pH = 7,0, dried over anhydrous sodium sulfate, the solvent was removed at 10 mm. Hg.

Synthesis of methyl esters of N-Dns-[2H, 13C] amino acids

Synthesis of methyl esters of N-Dns-[2H, 13C]amino acids was carried out with using diazomethane. For obtaining of diazomethane to 20 ml of 40% KOH dissolved in 40 ml of diethyl ether was added 3,0 g of wet nitrosomethylurea and stirred at ice-water bath for 15–20 min. After intensive gassing closure ether layer was separated, washed with ice water until pH = 7,0, dried over anhydrous sodium sulfate, and further used to treat N-[2H, 13C]-Dns-amino acids in composition of culture liquids and hydrolysates of total proteins of biomass.

Synthesis of N-Cbz-[2H, 13C] amino acids

For the synthesis of N-Cbz-[2H, 13C]amino acids to 1,5 ml cooled to 0 0C of culture liquid solution (50 mg) or protein hydrolyzate (5,4 mg) in 4 M NaOH were added in portions with stirring 2 ml of 4 M NaOH and 28,5 mg of benzyloxycarbonyl. The reaction mixture was kept at 0 0C, stirred for about 3 hours, acidified with 2 M HCl to pH = 3,0 and extracted with ethyl acetate (3×5 ml). The combined extract was washed with water until pH = 7,0, dried over anhydrous sodium sulfate, the solvent was removed at 10 mm. Hg.

Methods for analytical determination of
2H- and 13C-labeled amino acids and proteins

TLC of derivatives of 2H- and 13C-labeled amino acids was performed on plates with Silufol UV-254 ("Kavalier", Slovakia) in solvent systems: chloroform–methanol–acetic acid, 10:1:0,3, vol.% (A) for N-Cbz-[2H, 13C]amino-acids, and methanol–chloroform–acetone, 7:1:1, vol.% (B) for methyl esters of N-Dns-[2H, 13C] amino asids. N-Cbz-[2H, 13C]amino acids were detected by UV absorbance at λ = 254 nm. Methyl esters of N-Dns-[2H, 13C]amino acids were detected by their fluorescence in UV light. Secreted L-phenylalanine and L-leucine were determined with a spectrophotometer Beckman DU- 6 ("Beckman Coulter", USA) at λ = 540 nm in 10 ml samples of liquid culture (LC) after the treatment with 1% of ninhydrin. The electrophoresis of bacteriorhodopsin was performed in 12,5% PAGE with 0,1% SDS. The samples for electrophoresis were prepared by standard method (protocol of LKB Company, Sweden). For the quantitative determination of the protein synthesized in the cell, the scanning was conducted in solution with Coomassie blue R-250 using a gel electrophoretic laser densitometer CDS-200 (Beckman Coulter, USA).

Analytical and preparative separation of
methyl esters of N-Dns-[2H, 13C] amino acids

Analytical and preparative separation of the mixture of methyl esters of N-Dns-[2H, 13C] of amino acids from the culture liquid and protein hydrolysates was carried out at t = 20±25 0C by RP HPLC on a liquid chromatograph Knauer Smartline (Knauer, Germany) equipped with a UV detector UF-2563 and integrator-R 3A (Shimadzu, Japan) using 250×10 mm column with the

stationary phase of Separon SGX C18, 7 μm (Kova, SK); mobile phase: (A) acetonitril–trifluoroacetic acid = 100:0,1–0,5 vol.% and (B) acetonitrile = 100 vol.% under the gradient elution conditions; sample volume – 50–100 μl; elution rate – 1,5 ml/min. The yield of methyl esters of the individual N-Dns-[2H, 13C] amino acids was 75–89%; the chromatographic purity – 95–98%.

Ion exchange chromatography of protein hydrolysates

Ion exchange chromatography of protein hydrolysates was performed on a Biotronic LC 5001 apparatus ("Eppendorf-Nethleler-Hinz", Germany) using a column with Biotronic resin BIC 2710; t = 20±25 0C; 3,2×230 mm; stationary phase: sulfonated styrene (7,25 % of cross-linking) resin UR-30 (Beckman Spinco, USA); mobile phase – 0,2 M Na-citrate buffer; operating pressure – 50–60 atm; feed rate of Na-citrate buffer – 18,5; ninhydrin – 9,25 ml/h; detection at λ = 570 nm and λ = 440 nm (for proline).

Mass spectrometry derivatives [2H, 13C]amino acids

Mass spectra of electron impact of [2H, 13C]amino acid derivatives were recorded on a MB-80 A (Hitachi, Japan) with a double focusing with ionizing voltage of 70 eV, an accelerating voltage of 8 kV and the temperature of the cathode source of 180–200 0C. The scanning of samples was analyzed at a resolution of 7500 arbitrary units using 10% image sharpness.

Results and discussions

Isolation of 2H and 13C -labeled amino acids from culture liquids and protein hydrolysates

The objects of the study were obtained by mutagenesis of L-phenylalanine-producing strain of the facultative methylotrophic bacteria Brevibacterium methylicum, assimilating methanol via xylulose-5-monophosphate cycle of carbon assimilation, and L-leucine-producing strain of obligate methylotrophic bacteria Methylobacillus flagellatum, implements a 2-keto-3 -deoxy-gluconate aldolase variant of ribulose-5-monophosphate cycle of carbon assimilation. To compensate auxotrophy for L-leucine and L-isoleucine, these amino acids were added into the growth medium in the protonated form. The levels of accumulation of L-phenylalanine and L-leucine in liquid cultures (LC) of these strains-producers reached values of 0,8 and 1,0 g/l respectively [18, 19]. The inclusion of deuterium into the molecules of secreted amino acids and total proteins was carried out via the cultivation of the strain of B. methylicum on mineral M9 medium with 2H2O and protonated methanol, as the level of inclusion of 2H into the amino acid molecules due to assimilation of [2H]methanol is negligible.

Since the cell assimilates hydrogen (deuterium) atoms from H2O (2H2O) environment, we selected conditions of deuterium enrichment of amino acid molecules and proteins under a stepwise increase in concentration of 2H2O in growth media as shown in Table 1. The growth of microorganisms on 2H2O containing growth media was characterized by increasing the duration of the lag phase, the cell generation time, and the reduction of outputs of the microbial biomass (Table 1), so it was necessary to carry out the adaptation of cells to 2H2O.

The method of the optional adaptation of the strain of methylotrophic bacteria B. methylicum to grow on 2H2O while maintaining the ability for the biosynthesis of L-phenylalanine was described in article [20]. In this research, were investigated samples of the culture liquids and biomass hydrolysates obtained during the multi-stage adaptation of B. methylicum to heavy water on minimal mineral M9 media with the different content of 2H2O (from 24,5 to 98,0% 2H2O). Since this strain of methylotrophic bacteria was adapted to grow in 2H2O, the study of inclusion levels of deuterium into the amino acid molecules was the most interesting.

Unlike the bacterial growth on 2H2O medium, wherein it was necessary to carry out the cell adaptation to deuterium, at the preparation of [13C]amino acids via assimilation of 13CH3OH this stage was not required because this isotopic substrate does not exert the adverse biostatic effect on the growth characteristics of methylotrophs (Table 1). Therefore, in the case of the strain of obligate methylotrophic bacteria M. flagellatum the inclusion of 13C into amino acid molecules was carried out in one step by growing the bacteria on minimal M9 media containing 1% of [13C]methanol as a source of carbon-13 isotope.

Table 1: The influence of the isotopic composition of growth media on the growth of strains of B. methylicum and M. flagellatum

Number of experiment	Growth media*	The value of lag-phase, h	The output of biomass, % from control	The generation time, h
1	0	24,0	100	2,2
2	24,5	32,1	90,6	2,4
3	49,0	40,5	70,1	3,0
4	73,5	45,8	56,4	3,5
5	98,0	60,5	32,9	4,4
6	CH3OH	0	100	1,1
7	13CH3OH	0,1	72,0	1,0

Notes:
* Data for experiments 1–5 were presented for B. methylicum while growing on aqueous M9 media containing 2% methanol and a specified amount (vol.%) of 2H2O. Data for experiments 6–7 show for M. flagellatum when growing on aqueous M9 media containing 1% methanol (6) or 1% [13C] methanol.

As another model system for inclusion of isotopic label into the protein molecules used a transmembrane protein bacteriorhodopsin [21] synthesized in the purple membrane of extreme photo-organotrophic halobacterium Halobacterium halobium ET 1001. The selection for this purpose of bacteriorhodopsin functioning in halobacteria cells as the ATP-dependent translocase was dictated by the ability to use it to study of the functioning of membrane proteins in vivo in deuterium isotope enriched media. To include the deuterium label into the bacteriorhodopsin molecule used a method for the selective enrichment of protein by deuterium at functionally important residues of aromatic amino acids – phenylalanine, tyrosine and tryptophan due to the growing of halobacterium H. halobium ET 1001 on mineral synthetic medium containing the deuterated analogues of aromatic amino acids – L-[2,3,4,5,6-2H]phenylalanine, L-[3,5-2H]tyrosine and L-[2,4,5,6,7-2H]tryptophan.

The main stages for the isolation of [2H, 13C]amino acids involved the growing of respective strains producers on growth media containing labeled substrates – [2H]methanol, [13C]methanol and 2H2O or L-[2,3,4,5,6-2H]phenylalanine, L-[3,5-2H]tyrosine and L-[2,4,5,6,7-2H]tryptophan (bacteriorhodopsin), isolation of culture liquids (CL) containing [2H, 13C]amino acids from microbial biomass, purification of lipids, cell disruption, isolation of fraction of total protein of biomass and bacteriorhodopsin with their subsequent hydrolysis, derivatization of mixtures of amino acids by dansyl chloride, benzyloxycarbonyl chloride and diazomethane, separating of methyl esters of N-Dns-amino acid derivatives and N-Cbz-amino acid derivatives by reversed-phase HPLC and EI mass spectrometry of the obtained [2H, 13C]amino acid derivatives.

2H and 13C-labeled amino acids were isolated from lyophilized culture liquids of amino acid producing strains of B. methylicum and M. flagellatum, and as part of the total protein hydrolysates of microbial biomass. When isolating the total protein fraction it should be considered the presence of carbohydrates, lipids and pigments in samples. We used the protein rich bacterial strains with a relatively low content of carbohydrates in them. As a fraction of the total protein in the hydrolysis was subjected the residue obtained after the separation of exhaustive extraction of lipids and pigments by organic solvents (methanol–chloroform–acetone). In rare cases for the complete separation of the cellular components used the colloidal dissolution (solubilization) of proteins in 0,5% of SDS, or the salting out by ammonium sulfate.

The isolation and purification of individual proteins to further investigate their spatial structure can be advantageously carried out by the colloidal dissolving (solubilization) with using suitable detergents [22] that is especially important for bacteriorhodopsin which is a highly spiral transmembrane protein. Therefore, while separating of bacteriorhodopsin from purple membranes of halobacterium H. halobium ET 1001 used the solubilization of a purple membrane fraction after the washing out from extraneous phospholipids and carotenoids by 0,5% solution of SDS with preserving of α-helical configuration of the protein, and further precipitation of the protein from

DNS solution with methanol. The homogeneity of the isolated bacteriorhodopsin was confirmed by electrophoresis in 12,5% PAGE with 0,1% SDS.

The hydrolysis of 2H-labeled proteins was performed under conditions to prevent hydrogen isotopic exchange reactions with deuterium during the hydrolysis and preservation of the aromatic [2H]amino acid residues in the protein. We considered two alternatives variants – the acid and alkaline hydrolysis. The acid hydrolysis of the protein under standard conditions (6 M HCl, 24 h, +110 0C), is known to induce complete degradation of tryptophan and partial degradation of serine, threonine, and several other amino acids in the protein [23]. Another significant drawback when carrying out the hydrolysis in HCl consists in the isotopic (1H–2H) exchange of aromatic protons (deuterons) in molecules of tryptophan, tyrosine and histidine, as well as protons (deuterons) at the C3 atom of aspartic and C4 glutamic acids [24]. Therefore, to obtain the information about the real inclusion of deuterium into biosynthetically synthesized molecules of amino acids it was necessary to carry out the protein hydrolysis in deuterated reagents (6 M 2HCl with 3% phenol (in 2H2O)).

Another variant of hydrolysis of the protein was consisted in using 2 M Ba(OH)2 (+110 0C, 24 h). Under these conditions the reactions of isotopic (1H–2H) exchange at aromatic [2H] amino acids – tyrosine and tryptophan do not occur, and tryptophan is not destroyed. Both these methods of hydrolysis showed good results for the conservation of aromatic [2H]amino acids in the protein hydrolysate and the content of deuterium into the molecules of [2H]amino acids. It must be emphasized, however, that for the preparative production of 2H-labeled amino acids from the microbial protein is advisable to use the hydrolysis in 2HCl in 2H2O (in the presence of phenol to maintain the aromatic amino acid) to prevent racemization. For studying the enrichment level of stable isotopes inclusion into residues of aromatic [2H]amino acids of bacteriorhodopsin and for analytical purposes it is better to use the hydrolysis of protein in the solution of Ba(OH)2, in which there is no isotopic (1H–2H) exchange in amino acids and the residues of [2H]phenylalanine, [2H]tyrosine and [2H]tryptophan are retained in the protein. The possible D,L-amino acid racemization by alkaline hydrolysis did not affect the result of the subsequent mass spectrometric study of the level of deuteration into [2H]amino acid molecules.

For preparation of volatile derivatives the amino acids were converted into the methyl esters of N-Dns-[2H, 13C]amino acids or N-Cbz-[2H, 13C]amino acids, which were further separated by RP HPLC method. The conditions of N-derivatization of [2H, 13C]amino acids were practiced so as to obtain as much as possible intensive the molecular ion peaks (M+.) in EI mass spectra at the background level of the growth media metabolites. For this it was carried out the direct N-derivatization of [2H, 13C]amino acids in the composition of lyophilized culture liquids and total protein hydrolysates of biomass by 5-fold excess of dansyl chloride (in acetone) or benzyloxycarbonyl.

Under conditions of the reaction of N-derivatization for lysine, histidine, tyrosine, serine, threonine and cysteine along with monoderivatives were formed N-di-Dns and N-di-Cbz-derivatives. In addition, from arginine it was synthesized N-three-Dns-(Cbz)-arginine. Therefore, in mass-spectrometric studies the molecular ions (M+.) of these compounds were corresponded to di- or tri-derivatives.

The effectiveness of the use of N-Cbz- and N-Dns-amino acid derivatives in the RP-HPLC and EI mass spectrometric studies was demonstrated by us previously [25]. The volatility of N-derivatives of amino acids in EI mass spectrometric analysis can be further enhanced by the esterification of the carboxyl group, so that N-Dns-[2H, 13C]amino acids were converted into their methyl esters. To prevent the reverse isotopic exchange of aromatic protons (deuterons) in a process of esterification of 2H-labeled amino acids, in this research we gave a preference to diazomethane. The freshly prepared solution of diazomethane in diethyl ether was treated with dry mixtures of amino acids residues. At derivatization of amino acids with diazomethane it was occurred an additional N-methylation at α-NH-(Dns)-group in [2H]amino acids, leading to the appearance in the EI mass spectra of methyl esters of N-Dns-amino acids the additional peaks corresponding to compounds with a molecular mass on 14 mass units larger than the original compounds.

Study of levels of inclusion of stable isotopes of 2H and 13C into molecules of amino acids and hydrolysates

The levels of inclusion of stable isotopes of 2H and 13C into multicomponent mixtures of amino acid molecules of culture liquids and protein hydrolysates were determined analytically by EI mass spectrometry method. According to the mass spectrometric analysis the molecular ion peaks [M]+ of methyl esters of N-Dns-[2H]derivatives of aromatic [2H]amino acids have a low intensity in EI mass spectra and were polymorphously split, so the areas of the molecular enrichment were strongly broadened. Moreover, mass spectra of the mixture components are additive, so the mixture can be analyzed only if the spectra of the various components are recorded under the same conditions. These calculations provide for the solution of the system of n equations in n unknowns for a mixture of n components. For components, the concentration of which exceeds 10 mol.%, the accuracy and reproducibility of the analysis makes up ±0,5 mol.% (at 90% confidence probability). Therefore, to obtain reproducible results on deuteration levels it was necessary to chromatographically isolate individual derivatives of [2H] amino acids from the protein hydrolyzate. Methyl esters of N-Dns-[2H, 13C]amino acid derivatives or N-Cbz-[2H, 13C]amino acid derivatives were separated by The method of preparative RP-HPLC on octadecylsilane gel Separon SGX C18. The best result on separation was achieved by gradient elution of the methyl esters of N-Dns-[2H, 13C]amino acid derivatives with a mixture of solvents: (A) – acetonitril–trifluoroacetic acid = 100:0,1–0,5 vol.% and (B) – acetonitrile 100 vol.% in the gradient elution conditions by gradually increasing the concentration of component B in the mixture from 0 to 100 %. In this case, each component of the mixture was separated in the most optimal composition of the eluent, thereby achieving their full separation quality in much less time than in isocratic mode. In addition, using the gradient was significantly increased the maximum number of peaks in the chromatogram can accommodate – a peak capacity, which is very important in the separation of complex multi-component mixtures, which are the protein hydrolysates. Thus, it was possible to separate the tryptophan and intractable pair of phenylalanine/tyrosine by this method. The degrees of chromatographic purity of 2H- and 13C-labeled amino acids, isolated from culture liquids of B. methylicum and M. flagellatum and protein hydrolysates in the form of their N-Cbz-[2H, 13C]amino acid derivatives comprised 96–98% with yields – 67–89%. For some [2H, 13C]amino acids was proved to be more convenient the separation as methyl esters of N-Dns-[2H, 13C] amino acid derivatives. The degrees of the chromatographic purity of methyl esters N-Dns-[2H]phenylalanine, N-Dns-[2H]tyrosine and N-Dns-[2H]tryptophan obtained from the hydrolysates of bacteriorhodopsin were 96, 97 and 98%, respectively. This result is important because of the chemical stability of methyl esters of N-Dns-amino acids; the presence of high-molecular ions (M+.) at higher molecular weights have proved to be very convenient for mass spectrometric investigations and enable to identify 2H- and 13C-labeled amino acids in the presence of low molecular weight metabolites in growth media and other products of derivatization. The latter fact is very important to study the composition of the pool of 2H- and 13C-labeled amino acids secreted into the culture liquids of amino acid producing strains and total protein hydrolysates.

The fragmentation pathways of methyl esters of N-Dns-phenylalanine and N-Dns-leucine by the electron impact mass spectrometry lead to the formation of molecular ion peaks (M+.) at m/z = 412 and m/z = 378 and to the formation of dansyl fragments and products of the further decay to N-dimethylaminonaphthalene, and the formation of the amine fragment A+ and aminoacyl fragment B+ (Fig. 1). The fragmentation of methyl esters of N-Dns-phenylalanine and N-Dns-leucine shown on Fig. 1 is typical for these derivatives of all other amino acids, which allows carry out the mass spectrometric monitoring of 2H- and 13C-labeled amino acids in the intact culture liquids of producing strains containing in liquid media the amino acid mixtures and other metabolites of the growth medium until the stage of chromatographic separation, as well as explore the inclusion of stable isotopes of 2H- and 13C into the molecules of amino acids of protein hydrolysates.

Table 2: The results of one-step gradient separation of a mixture of methyl esters of N-Dns-[2H, 13C]amino acids from hydrolysates by RP HPLC, t = 20±25 0C on a 250×10 mm column with octadecylsilane gel Separon SGX C18, 7 μ (Kova, Slovakia)

Number of processing	Components of the mobile phase, vol.%		Elution time
	A*	B**	
1	90	10	10
2	80	20	10
3	60	40	10
5	50	50	10
6	30	60	5
8	20	80	5
9	10	90	5
10	0	100	5

Notes:
* A – acetonitrile–trifluoroacetic acid = 100:0,1–0,5 vol.%
** B – acetonitrile = 100 vol.%

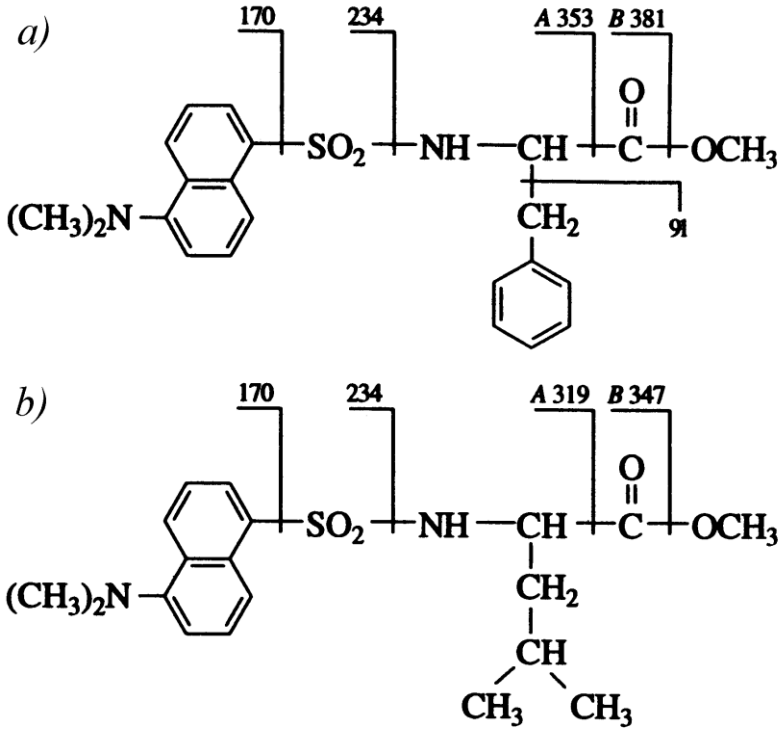

Figure 1: Fragmentation of methyl esters of N-Dns-phenylalanine with Mr = 412 (a) and N-Dns-leucine Mr = 378 (b) in the electron impact mass spectrometry method

When using as a source of stable isotopes [13C]methanol and 2H2O in the cell are synthesized the isotopically-substituted amino acids differ in the number of atoms substituted on isotopes of 13C and 2H. At the same time, the higher is the molecular weight of the amino acids, the larger is a set of possible molecular ions (M+.) corresponding to isotope-substituted forms. The peaks at m/z = 323,2; 337,4; 368,5; 382,3; 420,5 in the EI mass spectrum of [13C]amino acid derivatives in the derivatized liquid culture (LC) of M. flagellatum, obtained on aqueous medium with 1% [13C] methanol (Fig. 2b) correspond by the mass/charge ratios (m/z) to methyl esters of

N-Dns-[13C]glycine, N-Dns-[13C]alanine, N-Dns-[13C]valine, N-Dns-[13C]leucine/[13C]isoleucine and N-Dns-[13C] phenylalanine. It should be emphasized that the value of m/z for the molecular ion (M+.) of methyl esters of N-Dns-[13C]leucine and [13C]isoleucine in the EI mass spectra is the same, so these amino acids could not be accurately identified by this method. The maximum levels of inclusion of 13C isotope into amino acid molecules as measured by an increase of the averaged values of mass to charge ratio m/z for molecular ions (M+.) of isotopically-labeled sample in comparison with a molecular weight of a non-labeled natural amino acid are varied from 35% for [13C]alanine to 95% for [13C] phenylalanine (Fig. 2). Considering the auxotrophy of this strain for L-isoleucine, the variations in the range can be explained by the contribution of an exogenous isoleucine to the level of isotopic incorporation of [13C]leucine, and other metabolically related amino acids – [13C]alanine and [13C]valine.

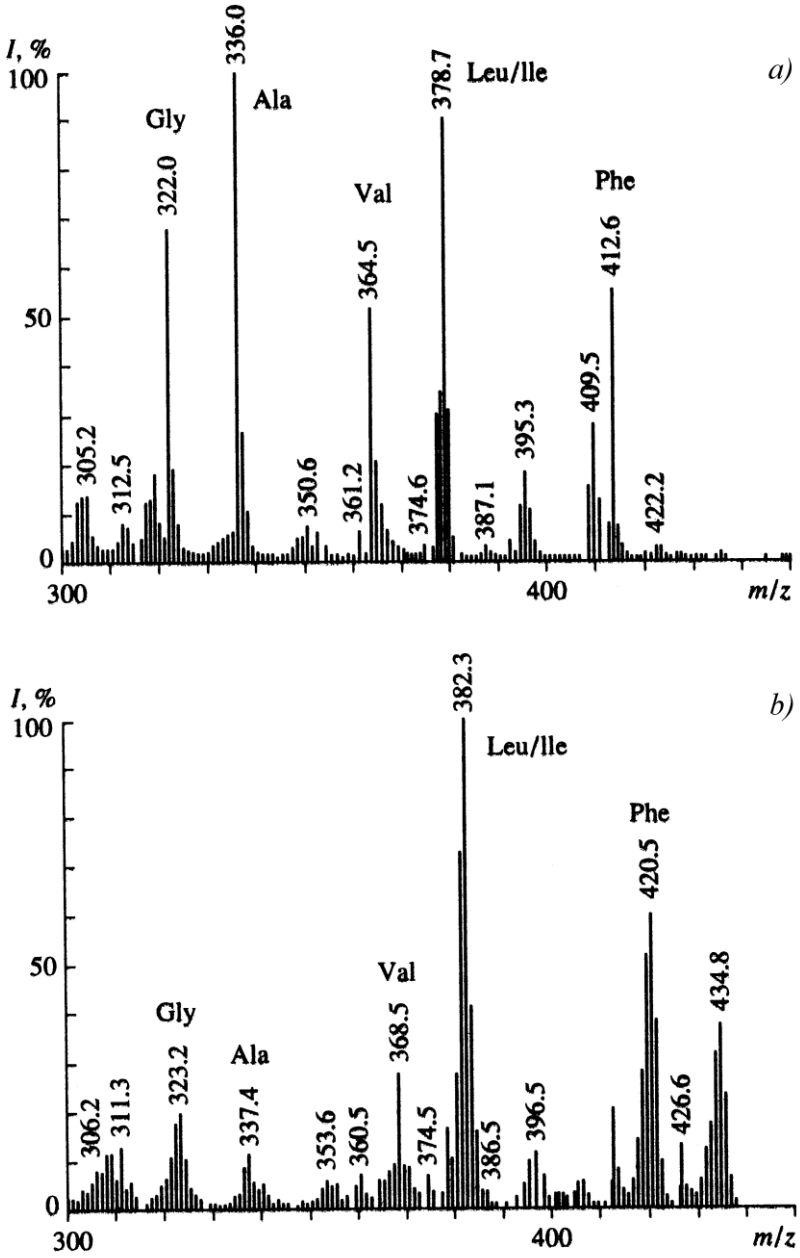

Figure 2: EI mass spectra of methyl esters of N-Dns-[13C]-amino acids from LC of M. flagellatum after treatment with diazomethane and dansyl chloride: a) – 1% methanol and H2O (control); b) – 1% [13C] methanol and H2O. Symbols of amino acids are marked peaks of molecular ions [M]+ of methyl esters of N-Dns-[13C] amino acids. The intensity of the peaks is given in %.

For the strain of methylotrophic bacteria B. methylicum there was a specific increase in the levels of isotopic incorporation of deuterium into molecules of individual [2H]amino acids in the composition of culture liquids (Table 3) with stepwise increasing concentrations of 2H2O in growth medium. The inclusion levels of deuterium into molecules of different [2H] amino acids under the same growing conditions are varied. In all experiments was observed the proportional increase in the levels of isotopic incorporation of 2H into the molecules of metabolically related [2H]amino acids with stepwise increasing concentrations of heavy water in the growth media (Table 3). This result was recorded in all experiments wherein as a source of stable isotopes was used 2H2O.

Table 3: Levels of 13C and 2H inclusion into molecules of amino acids (atom%), secreted into the culture liquid (CL) of B. methylicum and M. flagellatum, and into amino acid residues of protein

Amino acid	Content of 2H2O in the growth medium, %*								1% 13CH3OH**	
	24,5		49,0		73,5		98,0			
	LC	Protein	LC	Protein	LC	Protein	LC	Protein	LC	Protein
Glycine	–	15,0	–	35,0	–	50,0	–	90,0	60,0	90,0
Alanine	24,5	20,0	50,0	45,0	50,0	62,5	55,0	97,5	35,0	95,0
Valine	20,0	15,0	50,0	46,0	50,0	50,0	55,8	50,0	50,0	50,0
Leucine /Isoleucine	20,0	15,0	50,0	42,0	50,0	50,0	50,0	50,0	40,0	49,0
Phenylalanine	15,0	24,5	27,5	37,5	51,2	50,0	75,0	95,0	95,0	80,5
Tyrosine	–	20,0	–	25,6	–	68,5	–	92,8	–	53,5
Serene	–	15,0	–	36,7	–	47,6	–	86,6	–	73,3
Aspartic acid	–	20,0	–	36,7	–	60,0	–	66,6	–	33,3
Glutamic acid	–	20,0	–	40,0	–	53,4	–	70,0	–	40,0
Lysine	–	10,0	–	35,3	–	40,0	–	58,9	–	54,4

Notes:

* Data are submitted for inclusion of 2H into the amino acid molecules when growing of B. methylicum on aqueous M9 media containing 2% methanol and a specified amount (vol.%) of 2H2O.

** Data are submitted for inclusion of 13C when growing of M. flagellatum on aqueous M9 media containing 1% [13C]methanol.

From the mass spectrum of methyl esters of N-Dns-[2H]amino asid derivatives of culture liquid of B. methylicum, obtained on the growth medium containing 49% 2H2O (Fig. 3b) is shown that the phenylalanine molecule contains 6 isotopically-substituted forms with an average peak of molecular ion (M+.) with m/z = 414,2, which increases compared with the control conditions (m/z = 412,0, Fig. 3a) on 2,2 units, i.e. 27,5 atom.% of the total number of hydrogen atoms in the molecule are substituted with deuterium. The region in the mass spectrum with values m/z = 90–300 corresponds to relevant products of derivatization of metabolites in the growth medium. The peak with m/z = 431,0, recorded in the mass spectrum of the culture liquid manifested in all the experiments, corresponds to the product of additional methylation of the phenylalanine molecule at α-NH- (Dns)-group. The peak with m/z = 400 (Fig. 3b) corresponds to the product of cleavage of deuterated methyl group from the [2H]phenylalanine derivative.

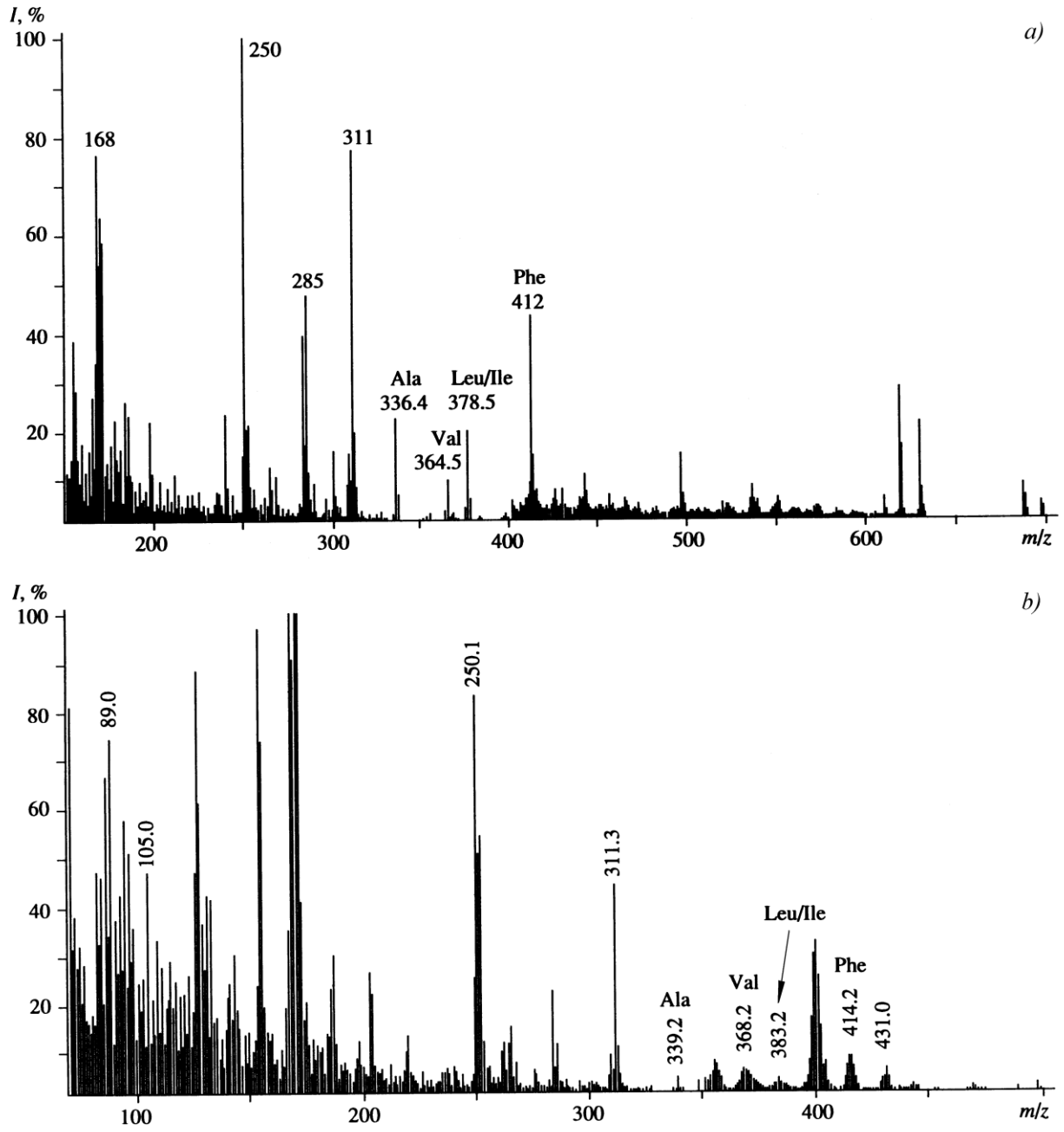

Figure 3: EI mass spectrum of methyl esters of N-Dns-[2H]-amino acids from LC of B. methylicum after treatment with diazomethane and dansyl chloride: a) – 2% methanol and 98,0% H2O (control); b) – 2% [2H]methanol and 49,0% of 2H2O

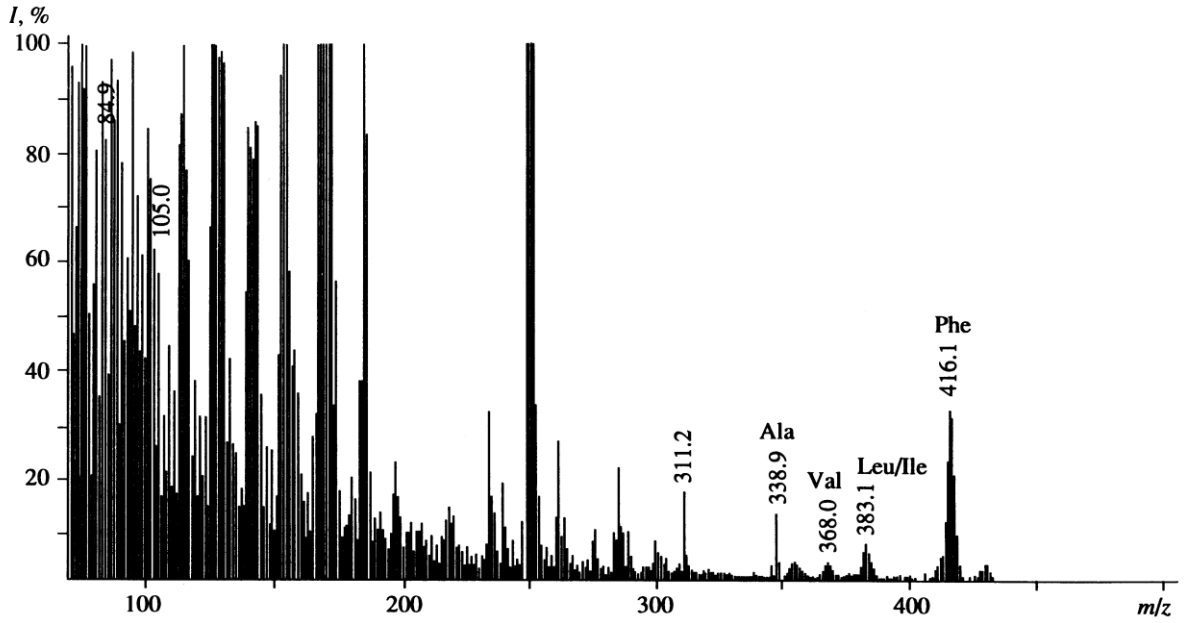

Figure 4: EI mass spectrum of methyl ester of N-Dns-[2H]-amino acids from CL of B. methylicum when grown on growth medium containing 2% [2H]methanol and 73,5% 2H2O

The presence in the EI mass spectrum of a sample of the liquid culture of B. methylicum, obtained on a medium containing 73,5% 2H2O (Fig. 4) the molecular ion peak of the methyl ester of N-Dns-[2H]phenylalanine (M+.) with m/z = 416,1 indicates on an increase in molecular weight of the [2H]phenylalanine molecule on 4,1 unit i.e. 51,2 % of hydrogen atoms in the molecule of [2H]phenylalanine in this case are replaced by deuterium. It is obvious that above mentioned deuterium atoms were entered into the [2H]phenylalanine molecule through biosynthesis de novo, i.e. into the carbon skeleton of the molecule. The protons (deuterons) at heteroatoms in the NH2- and COOH- groups of amino acids are appertained to the easily exchangeable ones, which are replaced by deuterium at the expense of their ease of the dissociation in H2O (2H2O) solutions.

From Table 3 it is shown that in conditions of auxotrophy in L-leucine the levels of inclusion of 2H into the molecules of [2H]leucine/[2H]isoleucine are lower than those ones for phenylalanine. This feature more clearly manifests in the medium with the highest concentration of 2H2O. Once again, this result is confirmed in Figure 5 that shows the EI mass spectrum of methyl esters of N-Dns-[2H]amino acids of liquid culture after the growth of the bacteria B. methylicum under these conditions. Clearly, the molecular ion peak of methyl ester of N-Dns-[2H]phenylalanyl (M+.) with m/z = 418,0 increases compared to control conditions for 6 units corresponding to the substitution of 75,0 atom.% of the total number of hydrogen atoms in the molecule. Unlike [2H] phenylalanine the inclusion level of deuterium enrichment in [2H]leucine/[2H]isoleucine was 50,0 atom.%, and [2H]valine – 58,8 atom.%. The peak with m/z = 432, recorded in the EI mass spectrum of methyl esters of N-Dns-[2H]amino acids of CL in Fig. 5 corresponds to additional methylation product of [2H]phenylalanine at α-NH2- group. In addition, in the EI mass spectrum is recorded the peak of the enriched with deuterium the benzyl fragment C6H5CH2 of [2H]phenylalanine with m/z = 97 (instead of m/z = 91 in the control), indicating that the sites of localization of six deuterium atoms in the molecule of [2H] phenylalanine are position of C1–C6 aromatic protons in the benzyl C6H5CH2 fragment. From mass spectrometry data is demonstrated that at other concentrations of 2H2O in growth media deuterium is also included in the aromatic ring of [2H]phenylalanine since the metabolism of the strain of B. methylicum adapted to 2H2O does not undergo significant changes in 2H2O [26].

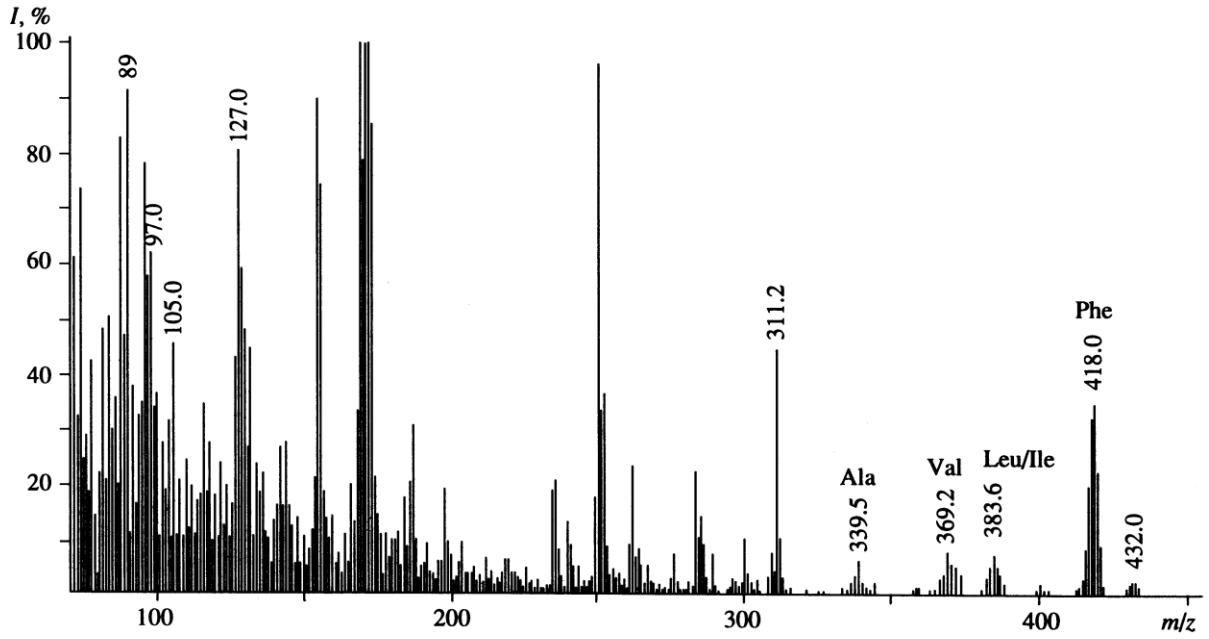

Figure 5: EI mass spectrum of methyl esters N-Dns-[2H]-amino acids from LC of B. methylicum when growing on the growth medium containing 2% [2H]methanol and 98,0% 2H2O (maximum deuterated M9-medium)

A similar pattern in inclusion levels of 13C isotope into amino acid molecules associated with auxotrophic metabolism was manifested when growing the L-isoleucine-dependent strain of M. flagellatum on the growth medium with 1% [13C] methanol. As can be seen from Table 3, unlike that observed for [13C]phenylalanine (the level of isotopic incorporation – 95,0%), the level of incorporation of 13C isotope into the molecules of [13C]leucine/[13C]isoleucine, [13C]alanine and [13C]valine were 38,0; 35,0 and 50,0% respectively. The level of isotopic incorporation into [13C]glycine (60%), was although higher than that for the last three amino acids, but significantly lower than that of [13C]phenylalanine.

Summarizing the data on the level of incorporation of 13C and 2H isotopes into secreted molecules of amino acids, it can be concluded about the maintaining of minor metabolic pathways associated with the de novo biosynthesis of leucine and the metabolically related amino acids. Another logical explanation for the observed effect, if we take into account the origin of leucine and isoleucine due to biosynthesis in various pathways (leucine belongs to the family of pyruvate, while isoleucine – to the family of aspartate (Fig. 6) could be the assimilation by the cell of the unlabeled leucine from the growth media under the background biosynthesis of isotopic-labeled isoleucine de novo. Taking into account of these effects it should be emphasized that the use of auxotrophic forms of microorganisms for production of 13C and 2H-labeled amino acids could not be justified practically because of the multiple character of inclusion of isotopes into the molecule [26]. On the contrary, the use for this purpose the prototrophic forms of microorganisms seem to be more promising for these aims.

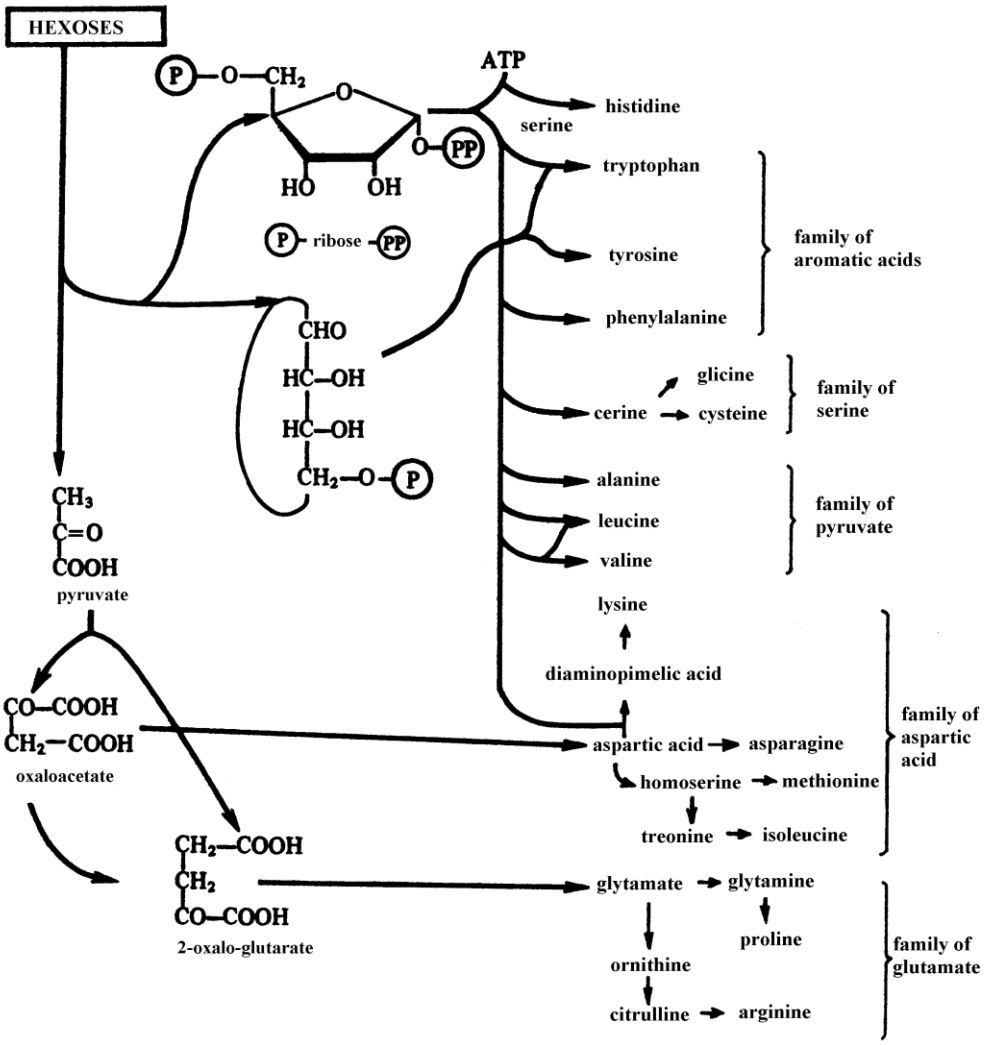

Figure 6: The amino acids required for the synthesis of proteins produced in cells from precursors (by G. Schlegel [27])

The general principles for the study of levels of isotope inclusion of molecules of amino acids in this method of labeling were exemplified by the analysis of complex multicomponent mixtures obtained after total hydrolysis of proteins of biomass of methylotrophic bacteria B. methylicum and transmembrane protein – bacteriorhodopsin, performing the role of ATP-dependent translocase in cells of photo-organotrophic halobacteria Halobacterium halobium. As seen in Figure 7, up until 10 amino acids may be identified in the protein hydrolysate of B. methylicum by peaks of molecular ions (M+.) of corresponding methyl esters of N-Dns-[2H]amino acid derivatives.

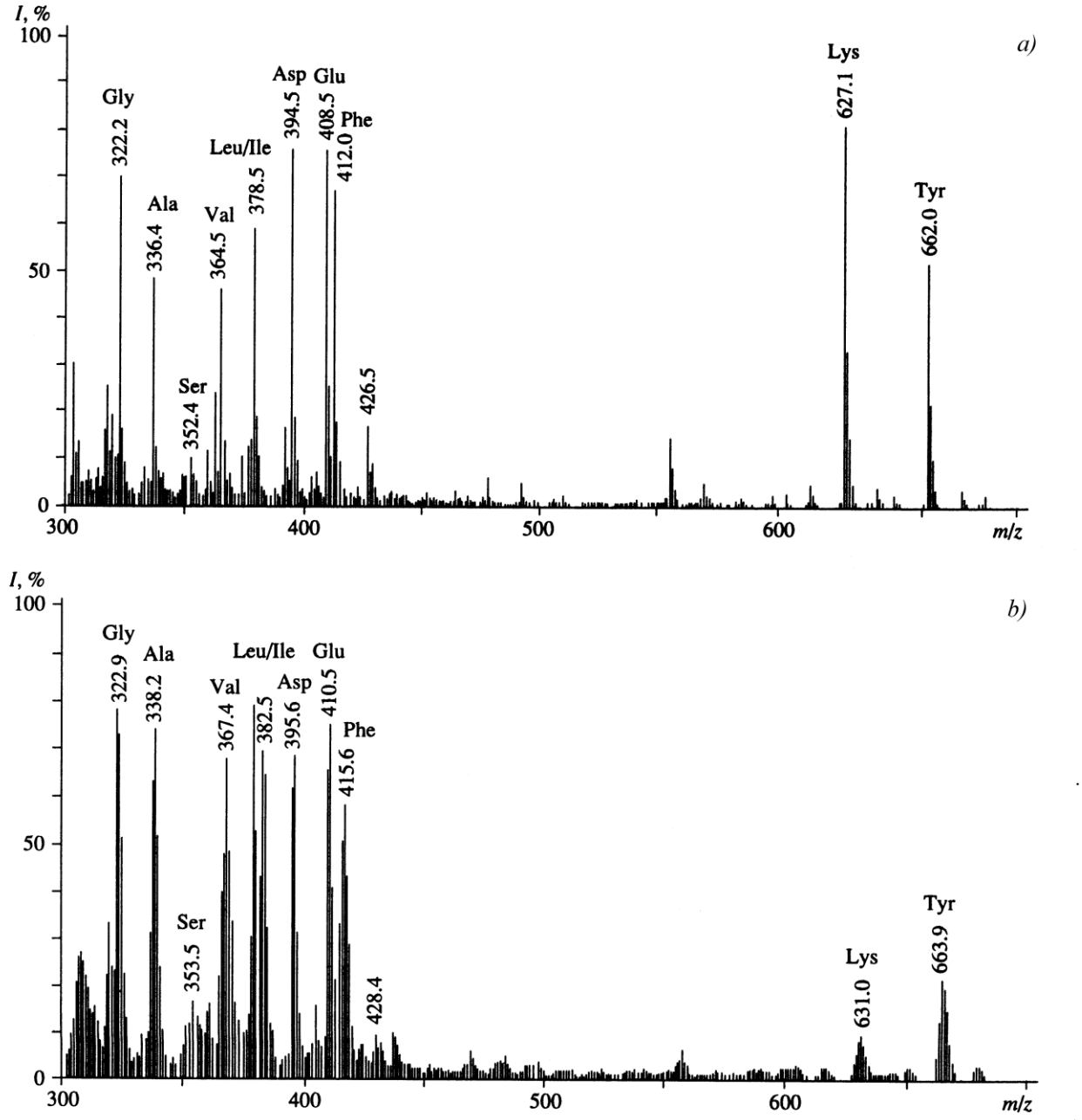

Figure 7: EI mass spectrum of methyl ester of N-Dns-[2H]-amino acids from hydrolysates of total protein of biomass of B. methylicum when growning on M9 medium, containing 2% methanol and H2O (control) (a) and 2% [2H]methanol and 98,0% 2H2O (b)

As in the case with secreted amino acids, the molecular ion peaks (M+.) were corresponded to isotopic mixtures of amino acid derivatives of isotopically substituted forms. For lysine and tyrosine the peaks (M+.) were corresponded to di-methyl esters of amino acid derivatives – α,ε-di-Dns-lysine ((M+.) at m/z = 631,0) and O,N-di-Dns-tyrosine ((M+.) at m/z = 663,9). The levels of isotopic incorporation of deuterium into the molecules of [2H]amino acids from the hydrolysate of total protein biomass at the 2H2O content in the growth medium from 49,0% to 98,0% were varied from 25,6% for [2H]tyrosine to 45,0% for [2H]alanine (Fig. 7b and Table. 3). The levels of isotopic incorporation of deuterium into the molecules of [2H]glycine, [2H]valine, [2H]phenylalanine, [2H]serine, [2H]lysine, [2H]aspartic and [2H]glutamic acid are raged within 35–46%. As in the case with secreted amino acids, with the increase of 2H2O concentration in growth media, it was observed the proportional increase in the level of incorporation of 2H isotope into amino acid molecules. With regard to other [2H]amino acids not detectable by this method, it is obvious that

the levels of isotope inclusion into the amino acid molecules are roughly the same. This is confirmed by data of separation of protein hydrolysates of methylotrophic bacteria by RP HPLC method as N-Cbz-[2H]amino acid derivatives and methyl esters of N-Dns-[2H]amino acid derivatives and ion-exchange chromatography of protein hydrolysates, wherein it is detected 15 amino acids (Fig. 8, Table 4).

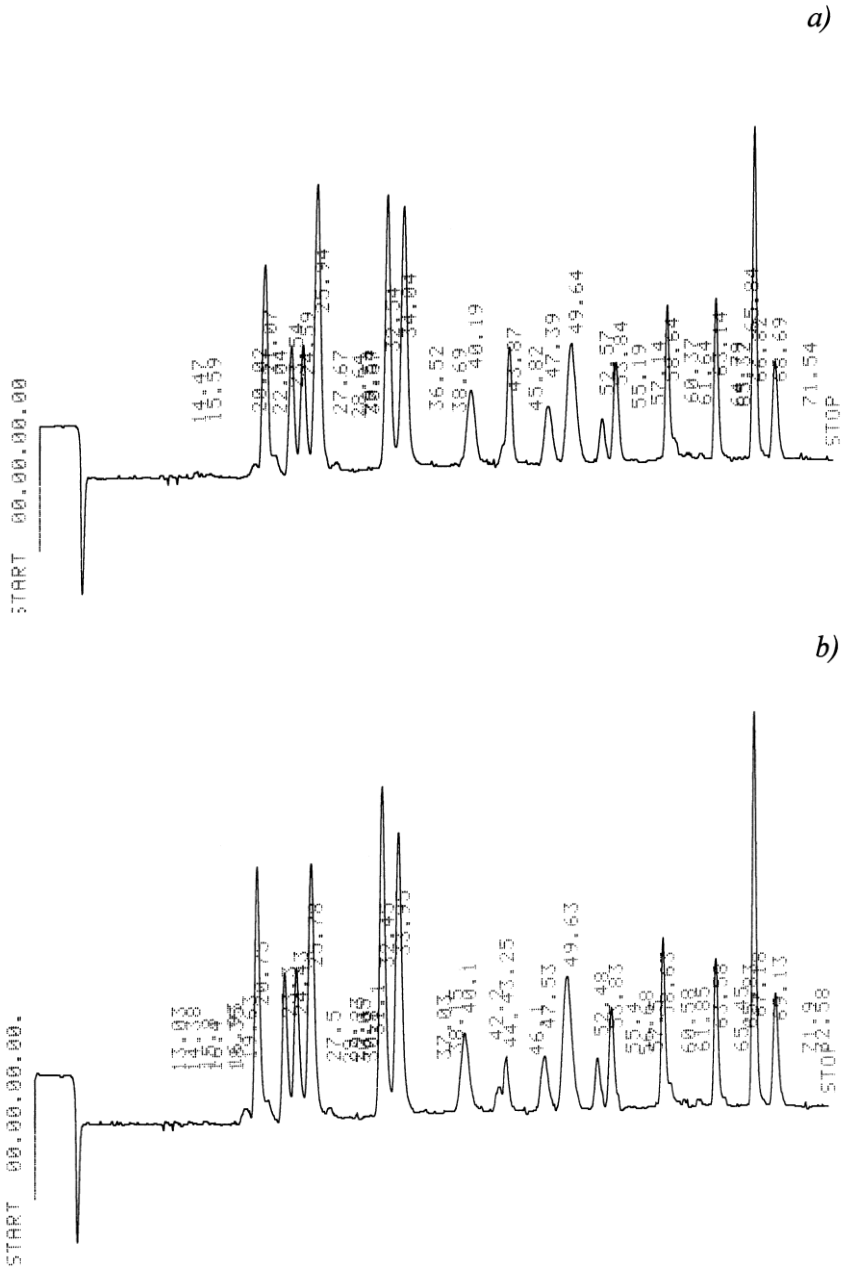

Figure 8: Ion exchange chromatography of amino acids from hydrolysates of protonated (a) and deuterated (b) cells of B. methylicum on maximum deuterated M9 medium: Biotronic LC-5001 (230×3,2 mm) (“Eppendorf-Nethleler-Hinz”, Germany); mobile phase: UR-30 sulfonated styrene resin ("Beckman-Spinco", USA); pellet diameter – 25 mm; working pressure – 50–60 atm; mobile phase – 0,2 M Na-citrate buffer (pH = 2,5); eluent flow rate – 18,5 ml/h; ninhydrin – 9,25 ml/h; detection at λ = 570 and λ = 440 nm (for proline).

Table 4: The amino acid composition of a protein hydrolyzate of total protein of biomass of B. methylicum, obtained in the maximum deuterated growth medium* and levels of deuterium enrichment of molecules **

Amino acid	Output, % of dry weight of biomass		The number of included deuterium atoms in carbon skeleton of the molecule	The deuterium enrichment level, % from a total number of hydrogen atoms***
	Protonated sample (control)	Deuterated sample obtained in 98,0% 2H2O		
Glycine	8,03	9,69	2	90,0
Alanine	12,95	13,98	4	97,5
Valine	3,54	3,74	4	50,0
Leucine	8,62	7,33	5	50,0
Isoleucine	4,14	3,64	5	50,0
Phenylalanine	3,88	3,94	8	95,0
Tyrosine	1,56	1,83	7	92,8
Serine	4,18	4,90	3	86,6
Threonine	4,81	5,51	–	–
Methionine	4,94	2,25	–	–
Aspartic acid	7,88	9,59	2	66,6
Glumatic acid	11,68	10,38	4	70,0
Lysine	4,34	3,98	5	58,9
Arginine	4,63	5,28	–	–
Histidine	3,43	3,73	–	–

Notes:
* Data obtained on M9 medium with 98,0% 2H2O and 2% [2H]methanol.
** When calculating the deuterium enrichment level protons (deuterons) at COOH and NH2 groups of amino acid molecules are not taken into account because of the ease of their dissociation and isotopic exchange in H2O/2H2O.
*** A dash indicates no data.

The findings suggest about the possibility of achieving maximum levels of inclusion of stable isotopes 2H and 13C into the amino acid residues of the total protein biomass (except for alanine, valine and leucine/isoleucine, reduced levels of inclusion of which explains the effect of auxotrophy for L-leucine and L-isoleucine). For example, in the case of the deuterated amino acid substitution at full stable isotopes has been achieved by using as a source of deuterium 98,0% 2H2O (Table 4). As can be seen from Table 4, when the growning of B. methylicum on growth medium with 98,0% 2H2O, the inclusion levels of 2H into residues of glycine, alanine, phenylalanine and tyrosine constitute 90,0; 97,5; 95,0 and 92,8 atom.%. In experiments on the inclusion of 13C isotope into the total protein biomass due to the assimilation of [13C]methanol by methylotrophic bacteria M. flagellatum were also observed high levels of isotopic incorporation in [13C]glycine (90,0%), [13C] alanine (95,0%) and [13C]phenylalanine (80,5%) (Table 3). As in the case with secreted amino acids the reduced inclusion levels of stable isotopes into [13C]leucine/isoleucine (49,0%), as well as into the related metabolic [13C]amino acids under these conditions could be explained by the effect of auxotrophy of the strain in L-isoleucine, which was added to the growth medium in the protonated form.

In all isotopic experiments on the integration of stable isotopes 2H and 13C into the amino acid molecules the levels of inclusion of 2H and 13C into metabolically related amino acids found a certain correlation. Thus, the isotopic incorporation levels for alanine, valine and leucine (pyruvate family), phenylalanine and tyrosine (aromatic amino acid family, synthesized from shikimic acid) are correlated (see Table 3). At the same time levels of isotope inclusion for alanine, valine and leucine/isoleucine are stable within a wide variation of 2H2O concentration due to the effect of auxotrophy on leucine. The levels of isotopic incorporation for glycine and serine (serine family),

aspartic acid, and lysine (asparagines family) also have similar values and are in correlation. Table 3 shows that the levels of isotopic incorporation into secreted amino acids and corresponding amino acid residues in the total protein when growing on media with the same isotope content generally are well correlated. The reason for some of the observed differences in the level of inclusion of isotopes into amino acid molecules can be associated with the effect of auxotrophy of the used strains in leucine and isoleucine.

This biosynthetic approach showed good results on the introduction of the deuterium label into the molecule of transmembrane protein bacteriorhodopsin, obtained via the growing of the photo-organotrophic halobacterium H. halobium on medium containing L-[2,3,4,5,6-2H] phenylalanine, L-[3,5-2H] tyrosin and L-[2,4,5,6,7-2H] tryptophan. The El mass spectrum of the mixture of methyl esters of N-Dns-[2H]amino acids as shown in Figure 9 (scanning at m/z = 50–640, base peak at m/z = 527, 100%), is characterized by continuity: the peaks in the range at m/z = 50–400 on the scale of the mass numbers are fragments of metastable ions, low molecular weight impurities, as well as products of chemically modified amino acids. The analyzed aromatic [2H]amino acids occupied the scale mass numbers at m/z = 415–456, are mixtures of molecules containing various numbers of deuterium atoms. Therefore, the molecular ions [M]+ were polymorphously split into individual clusters displaying a statistical set of m/z values depending on a number of hydrogen atoms in the molecule. Taking into account the effect of isotopic polymorphism, the level of deuterium enrichment in [2H]amino acid molecules was determined using the most commonly encountered peak of the molecular ion [M]+ in each cluster with mathematically averaged value of [M]+ (Fig. 9). Thus, for phenylalanine molecular ion peak was determined by [M]+ at m/z = 417, 14% (instead of the [M]+ at m/z = 412, 20% for non-labeled derivative (unlabeled peaks of amino acid derivatives are not shown)), tyrosine – [M]+ at m/z = 429, 15% (instead of [M]+ at m/z = 428, 13%), tryptophan – [M]+ at m/z = 456, 11% (instead of [M]+ at m/z = 451, 17%). The level of deuterium enrichment corresponding to the increase of molecular weight was for [2H]tyrosine 1 (90 atom.% 2H), [2H]phenylalanine – 5 (95 atom.%, 2H) and [2H]tryptophan – 5 (98 atom.% 2H) deuterium atoms. This result coincides with the data on the initial level of deuterium enrichment of aromatic amino acids – [3,5-2H2]Tyr, [2,3,4,5,6-2H5]Phe and [2,4,5,6,7-2H5]Trp, added to the growth medium and indicates a high selectivity of inclusion of aromatic [2H]amino acids into the BR molecule. Deuterium was detected in all residues of aromatic amino acids (Table 5). However, the presence in the EI mass spectrum the peaks [M]+ of protonated and semi-deuterated phenylalanine analogues with [M]+ at m/z = 413–418, tyrosine – with [M]+ at m/z = 428–430 and tryptophan – with [M]+ at m/z = 453–457 with different levels of contributions to the deuterium enrichment of molecules testifies about the conservation of the minor pathways of biosynthesis of aromatic amino acids de novo, resulting in the dilution of the deuterium label in molecules, that evidently is determined by the conditions of biosynthesis of 2H-labeled bacteriorhodopsin (Table 4). In addition to the above-mentioned amino acids in the EI mass spectrum are recorded molecular ion peaks of methyl ester of N-Dns-glycine ((M+.), m/z = 322), N-Dns-alanine ((M+.), m/z = 336), N-Dns-valine ((M+.), m/z = 364) and N-Dns-leucine/isoleucine ((M+.), m/z = 378). As might be expected, these amino acid residues in bacteriorhodopsin do not contain deuterium.

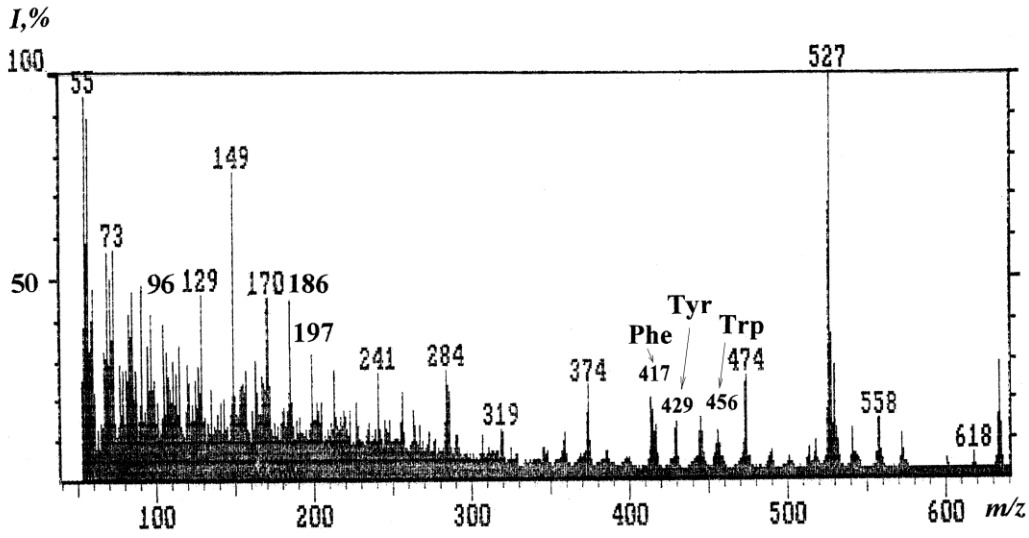

Figure 9: Full scan EI mass spectrum of methyl ester of N-Dns-[2H]derivatives of aromatic amino acids isolated from the hydrolysate of bacteriorhodopsin, obtained on the synthetic medium with L-[2,3,4,5,6-2H5]Phe (0,26 g/l), L-[3,5-2H2]Tyr (0,2 g/l) and L-[2,4,5,6,7-2H5]Trp (0,5 g/l) (energy: 70 eV, accelerating voltage: 8 kV, temperature: +180–200 0C). Hydrolysis conditions: 4 N Ba(OH)2 (in 2H2O), t = +110 0C, 24 h. Molecular ion peaks represented by the symbols of amino acids correspond to their derivatives; I – relative intensity (%).

Table 5: The values of the molecular ion peaks [M]+ in the EI mass spectrum of methyl esters of N-Dns-[2,3,4,5,6-2H5]Phe, N-Dns-[3,5-2H2]Tyr and N-Dns-[2,4,5,6,7-2H5]Trp and levels of their deuterium enrichment

Compound	Value of [M]+	Intensity, %	The total number of hydrogen atoms*	Level of deuterium enrichment, % of the total number of hydrogen atoms **
N-Dns-[2,3,4,5,6-2H5]Phe-OMe	413 414 415 416 417 418	7 18 15 11 14 6	1 2 3 4 5 6	13 25 38 50 63 75
N-Dns-[3,5-2H2]Tyr-OMe	428 429 430	12 15 5	– 1 2	– 14 29
N-Dns-[2,4,5,6,7-2H5]Trp-OMe	453 454 455 456 457	5 6 9 11 5	2 3 4 5 6	26 38 50 64 77

Notes:
* A dash means no incorporation of deuterium.
** In calculating the level of deuterium enrichment protons(deuterons) at carboxyl and NH2-amino groups of amino acids were not considered due to the easily isotopic (1H–2H) exchange.

Conclusion

The research has demonstrated the effectiveness of this method of biosynthesis of 2H- and 13C-labeled amino acids with different isotope enrichment levels, and electron impact mass

spectrometry of N-Cbz-amino acid derivatives and methyl esters of N-Dns-amino acid derivatives for the study of isotopic enrichment levels of [2H, 13C]amino acid molecules in composition of multicomponent mixtures obtained biosynthetically with using microorganisms. The method is indispensable for the study of a pool of amino acids, secreted into the culture liquid of producing strains grown on media with stable isotopes and protein hydrolysates of microbial biomass and may find further use in diagnostic studies.

This research was carried out with the financial support of the Research Center of Medical Biophysics (Bulgaria), grant number 112-RU.

References

1. Mosin O.V. Studying of methods of biotechnological preparation of proteins, amino acids and nucleosides, labeled with stable isotopes of 2H and 13C with high levels of isotopic enrichment, autoref. Cand chim. Nauk. Moscow: MSAFCT M.V. Lomonosov. 1996.

2. LeMaster D. M. Uniform and selective deuteration in two-dimensional NMR studies of proteins // Annu. Rev. Biophys. Chem. 1990. V. 19(2). P. 243–266.

3. MacCarthy P. Infrared spectroscopy of deuterated compounds: an undergraduate experiment // J. Chem. Educ. 1986. V. 62(7). P. 633–638.

4. Mosin O.V., Skladnev D.A., Egorova T.A., Shvets V.I. Mass-spectrometry evaluation of enrichment levels of 2H and 13C isotopes in molecules of bacterial objects // Bioorganic chemistry. 1996. V. 22, № 10–11. P. 856–869.

5. Crespi H. L. Biosynthesis and uses of per-deuterated proteins. Synthesis and Applications of Isotopically labeled Compounds. Proceedings of the Second International Symposium. New York: Elsevier. 1986. 115 p.

6. Mosin O.V., Skladnev D.A., Egorova T.A., Shvets V.I. Methods of preparation of amino acids and proteins, labeled with stable isotopes of 2H, 13C, 15N, 18O // Biotechnologija. 1996. № 10. P. 24–40.

7. Matthews H. R., Kathleen S., Matthews K., Stanley J. Selectively deuterated amino acid analogues. Synthesis, incorporation into proteins and NMR properties // Biochim. et Biophys. Acta. 1977. V. 497. P. 1–13.

8. LeMaster D. M., Cronan J. E. Biosynthetic production of 13C-labeled amino acids with site-specific enrichment // Journal of Biological Chemistry. 1982. V. 257. № 3. P. 1224–1230.

9. Mosin O.V., Ignatov I. Microbiological synthesis of 2H-labeled phenylalanine, alanine, valine, and leucine/isoleucine with different degrees of deuterium enrichment by the Gram-positive facultative methylotrophic bacterium Brevibacterium methylicum // International Journal of Biomedicine. 2013. V. 3. № 2. P. 132–138.

10. Mosin O.V., Shvets V.I., Skladnev D.A., Ignatov I. Microbial synthesis of deuterium-labeled L-phenylalanine by the facultative methylotrophic bacterium Brevibacterium meyhylicum on media with different concentrations of heavy water // Russian biopharmaceutical journal. 2012. V. 4, № 1. P. 11–22.

11. Patel G. B., Sprott G. D., Ekiel I. Production of specifically labeled compounds by Methanobacterium espanolae grown on H2-CO2 plus [13C]acetatet // Applied and Environmental Microbiology. 1993. V. 59. № 4. P. 1099–1103.

12. Mosin O.V., Shvets V.I., Skladnev D.A. Biosynthesis of transmembrane photochrome protein [2H]bacteriorhodopsin, labeled with deuterium at residues of aromatic amino acids [2,3,4,5,6-2H5]Phe, [3,5-2H2]Tyr and [2,4,5,6,7-2H5]Trp // Problems of biological, medicine and pharmaceutical chemistry. 2013. № 8. P. 29–39.

13. Mosin O.V., Shvets V.I., Skladnev D.A., Ignatov I. Microbial synthesis of 2H-labelled L-phenylalanine with different levels of isotopic enrichment by a facultive methylotrophic bacterium Brevibacterium methylicum with RuMP assimilation of carbon // Biochemistry (Moscow) Supplement Series B: Biomedical Chemistry. 2013. V. 7. № 3. P. 249–260.

14. Mosin O.V., Skladnev D.A., Shvets V.I. Introduction of deuterated amino acids in molecule of bacteriorhodopsine of Halobacterium halobium // Applied biochemistry and microbiology. 1999. Vol. 35. № 1. P. 34–42.

15. Neugebauer D.C., Zingsheim H.P., Oesterhelt D. Recrystallization of the purple membrane in vivo and in vitro // Journal Molecular Biology. 1978. V. 123. C. 247–257.

16. Oesterhelt D. The structure and mechanism of the family of retinal proteins from Halophilic Archaea Curr. Op. // Struct. Biol. 1988. V. 8. P. 489–500.

17. Bligh E. G., Dyer W. J. A rapid method for total lipid extraction and purification // Can. J. Biochem. Physiol. 1959. V. 37. № 8. P. 911–918.

18. Skladnev D.A., Mosin O.V., Egorova T.A., Eremin C.D., Shvets V.I. Methylotrophic bacteria – sources of источники isotopically labeled 2H- and 13C-amino acids // Biotechnologija. 1996. № 5. P. 25–34.

19. Karnaukhova E.N., Mosin O.V., Reshetova O.S. Biosynthetic production of stable isotope labeled amino acids using methylotroph Methylobacillus flagellatum // Amino Acids. 1993. V. 5. № 1. P. 125.

20. Mosin O. V., Skladnev D. A., Shvets V. I. Biosynthesis of 2H-labeled phenylalanine by a new methylotrophic mutant Brevibacterium methylicum // Bioscience, biotechnology, and biochemistry. 1998. V. 62(2). P. 225–229.

21. Mosin O.V., Ignatov I. Natural photo-transforming photo-chrome transmembrane protein bacteriorhodopsin from purple membranes of halobacterium Halobacterium halobium // Nano and microsystem technics. 2013. № 7. P. 47–54.

22. Ignatov I., Mosin O.V. Photoreceptors in visual perception and additive color mixing. Bacteriorhodopsin in nano- and biotechnologies // Advances in Physics Theories and Applications. 2014. V. 27. P. 20–37.

23. Cohen J. S., Putter I. The isolation of deuterated amino acids // Biochim. Biophys. Acta. 1970. V. 222. P. 515–520.

24. Penke B., Ferenczi R., Kovács K. A new acid hydrolysis method for determining tryptophan in peptides and proteins // Analytical Biochemistry. 1974. V. 60. № 1. P. 45–50.

25. Egorova T.A., Mosin O.V., Eremin C.B., Karnaukhova E.N., Zvonkova E.N., Shvets V.I. Separation of amino acid protein hydrolysates of natural objects by HPLC as carbobenzoxy derivatives // Biotechnologija. 1993. № 8. P. 21–25.

26. Mosin O.V., Ignatov I. Biological influence of deuterium on cells of prokaryotes and eukaryotes // Drugs development and registration. 2014. № 2(7). P. 122–131.

27. G. Schlegel. General Microbiology / ed. E.N. Kondrateva. Moscow: Mir. 1987. 255 p.

Published in the Russian Federation
European Reviews of Chemical Research
Has been issued since 2014.
ISSN: 2312-7708
E-ISSN: 2413-7243
Vol. 5, Is. 3, pp. 166-179, 2015

DOI: 10.13187/ercr.2015.5.166
www.ejournal14.com

UDC 541.64:574.24:553.08

Physical-Chemical Properties of Mountain Water from Bulgaria after Exposure To a Fullerene Containing Mineral Shungite and Aluminosilicate Mineral Zeolite

[1] Ignat Ignatov
[2] Oleg Mosin

[1] The Scientific Research Center of Medical Biophysics (SRC MB), Bulgaria
Professor, D. Sc., director of SRC MB
1111, Sofia, N. Kopernik street, 32
E-mail: mbioph@dir.bg
[2] Moscow State University of Applied Biotechnology, Russian Federation
Senior research Fellow of Biotechnology Department, Ph. D. (Chemistry)
103316, Moscow, Talalihina ulitza, 33
E-mail: mosin-oleg@yandex.ru

Abstract

We studied the physical-chemical properties of mountain water from Bulgaria influenced by the fullerene analogous, carbon containing natural mineral shungite from ***Zazhoginskoe deposit*** in Karelia (Russian Federation) and the microporous crystalline aluminosilicate mineral zeolite (Most, Bulgaria) for evaluation of the mathematical model of interaction of these minerals with water. The data about the structure and composition were obtained with using of transmission electron microscopy (TEM) and IR-spectroscopy. For evaluation of the mathematical model of interaction of these minerals with water, the methods of non-equilibrium spectrum (NES) and differential non-equilibrium spectrum (DNES) of water were applied. The average energy ($\Delta E_{H...O}$) of hydrogen H...O-bonds among individual molecules H_2O after treatment of shungite and zeolite with water was measured at -0,1137 eV for shungite and -0,1174 eV for zeolite. The calculation of $\Delta E_{H...O}$ for shungite with using DNES method compiles +0,0025±0,0011 eV and for zeolite -1,2±0,0011 eV. The results indicated on the different mechanisms of interaction of these minerals with water, which is determined by their structure and the composition of constituent components, resulting in a different physical-chemical behavior when interacting with water.

Keywords: shungite, zeolite, mountain water, IR-spectroscopy, NES, DNES

Introduction

Shungite and zeolite are minerals refer to new generation of natural mineral sorbents (NMS). Shungite is an intermediate form between the amorphous carbon and the graphite crystal, containing carbon (30 %), silica (45 %), and silicate mica (about 20 %) [1]. The schungite carbon is a fossilized organic material of sea bottom Precambrian sediments of high level of carbonization containing the fullerene-like regular structures. Shungite got its name after the village of Shunga in Karelia (Russian Federation), located on the shore of Onezhskoe Lake, where is located the only one mineral Zazhoginsky deposit of shungites on the territoty of the Russian Federation. The total

shungite researves of Zazhoginsky deposit amount to approximately 35 million tons of shungite. The plant production capacity for the mining and processing of shungite makes up 200 thousand tons of shungite per year.

Zeolites are the alumosilicate members of the family of microporous solids known as “molecular sieves”, named by their ability to selectively sort molecules based primarily on a size exclusion process. The natural zeolites form when volcanic rocks and ash layers react with alkaline groundwater. Zeolites also crystallize in post-depositional environments over periods ranging from thousands to millions of years in shallow marine basins. Naturally occurring zeolites are rarely pure and contaminated to varying degrees by other minerals, metals, quarts, or other zeolites. For this reason, naturally occurring zeolites are excluded from many important commercial applications where uniformity and purity are essential.

As natural minerales shungite and zeolite has unusually broad scope of application in industry. Shungite was used initially, mainly as a filler and substitute of the carbon coal coke (fuel) in blast furnace production of high-silicon cast iron, in ferroalloys melting, in the production of non-stick heat-resistant paints and coatings, and as filler in rubber production. Subsequently there were discovered other new valuable properties of shungite – adsorptional, bactericidal, catalytic, reduction-oxidation properties, as well as the ability of sungite minerals to screen off electromagnetic and radio radiations. These properties have made the use of shungite in various branches of science, industry and technology, for creating on its basis a variety of new nanotechnological materials with nano-molecular structure. On the basis of shuntite have been created new conductive paints, fillers for plastic materials, rubber and carbon black substitutes, composite materials, concrete, bricks, stuccoing plasters, asphalts, as well as materials having bactericidal activity, and materials shilding off the radio and electromagnetic radiation. Adsorptional, catalytic, and reduction-oxydation properties of shungite favored its use in water treatment and water purification technologies, i.g. in treatment of sewage waters from many organic and inorganic substances (heavy metals, ammonia, organochlorine compounds, petroleum products, pesticides, phenols, surfactants, etc.). Moreover, shungite has a strongly marked biological activity and bactericidal properties.

Zeolites as shungites are widely used in industry as desiccants of gases and liquids, for treatment of drinking and sewage water from heavy metals, ammonia, phosphorus, as catalyst in petrochemical industry for benzene extraction, for production of detergents and for extracting of radionuclides in nuclear reprocessing. They are also used in medicine as nutritional supplements having antioxidant properties.

A wide range of properties of shungite and zeolite defines the search for new areas of industrial application of these minerals in science and technology that contributes to a deeper study of the structure with using the modern analytical methods. This paper is a continuation of our studies aimed at the investigation of physical-chemical properties of mountain water from Bulgaria influenced by shungite and the zeolite for evaluation of the mathematical model of interaction of these minerals with water.

Material and Methods

Material

The study was performed with samples of shungite obtained from Zazhoginsky deposit (Karelia, Russia) and zeolite (Most, Bulgaria). Samples were taken *and* analyzed in solid samples according to National standard of the Russian Federal Agency of Technical Regulation and Metrology. Samples were put into 100 cm^3 hermetically sealed glass tubes after being washed in dist. H_2O and dried in crucible furnace, and homogenized in homogenizer by mechanical grinding. For the decomposition of the shungite samples a system of microwave decomposition was used. Other methods of samples processing were watching with dist. H_2O, drying, and homogenization on cross beater mill Retsch SK100 (“Retsch Co.”, Germany) and Pulverisette 16 (“Fritsch GMBH”, Germany).

Analytical methods

The analytical methods were accredited by the Institute of Geology of Ore Deposits, Petrography, Mineralogy, and Geochemistry (Russian Academy of Sciences). Samples were treated by various methods as ICP-OES, GC, and SEM. Gas-chromatography (GC) was performed at Main

Testing Centre of Drinking Water (Moscow, the Russian Federation) on Kristall 4000 LUX M using Chromaton AW-DMCS and Inerton-DMCS columns (stationary phases 5 % SE-30 and 5 % OV-17), equipped with flame ionization detector (FID) and using helium (He) as a carrier gas.

Inductively coupled plasma optical emission spectrometry (ICP-OES)

The mineral composition of shungite was studied by inductively coupled plasma optical emission spectrometry (ICP-OES) on Agilent ICP 710-OES (Agilent Technologies, USA) spectrometer, equipped with plasma atomizer (under argon stream), Mega Pixel CCD detector, and 40 MHz free-running, air-cooled RF generator, and Computer-optimized echelle system: the spectral range at 167–785 nm; plasma gas: 0–22,5 l/min in 1,5 l/min; power output: 700–1500 W in 50 W increments.

Gas-chromatography

The total amount of carbon (C_{total}) in shungite was measured according to the ISO 29541 standard using elemental analyzer CHS-580 ("Eltra GmbH", Germany), equipped with electric furnace and IR-detector by combustion of 200 mg of solid homogenized sample in a stream of oxygen at the temperature +1500 ^{o}C.

Transmission electron microscopy

The structural studies were carried out with using transmission electron microscopy (TEM) on JSM 35 CF (JEOL Ltd., Korea) device, equipped with X-ray microanalyzer "Tracor Northern TN", SE detector, thermomolecular pump, and tungsten electron gun (Harpin type W filament, DC heating); working pressure: 10^{-4} Pa (10^{-6} Torr); magnification: 300000, resolution: 3,0 nm, accelerating voltage: 1–30 kV; sample size: 60–130 mm.

IR-spectroscopy

IR-spectra of shungite were registered on IR spectrometer Brucker Vertex ("Brucker", Germany) in KBr pellet probes of shungite (a spectral range: average IR – 370–7800 cm^{-1}; visible – 2500–8000 cm^{-1}; the permission – 0,5 cm^{-1}; accuracy of wave number – 0,1 cm^{-1} on 2000 cm^{-1}).

NES- and DNES-methods

NES- and DNES-methods were used for the estimation of energy of hydrogen bonds of shungite and zeolite solutions in water in order to evaluate the mathematical model of interaction of these minerals with water. The device measured the angle of evaporation of water drops from 72 ^{o} to 0 ^{o}. As the main estimation criterion was used the average energy ($\Delta E_{H...O}$) of hydrogen O...H-bonds between individual H_2O molecules in aqueous samples. NES-and DNES spectra of shungite and zeolite solutions in water were measured in the range of the energy of hydrogen bonds 0,08–0,387 eV or λ = 8,9–13,8 μm with using a specially designed computer program.

Results and Discussion

The composition and the structure of shungite and zeolite

According to the last structural studies shungite is a metastable allotropic form of carbon with high level of carbonization (carbon metamorhism), being on prior to graphite stage of coalification [2]. Along with carbon the shungite, obtained from Zazhoginsky deposit in Karelia (Russian Federation) contains SiO_2 (57,0 %), TiO_2 (0,2 %), Al_2O_3 (4,0 %), FeO (0,6 %), Fe_2O_3 (1,49 %), MgO (1,2 %), MnO (0,15 %), K_2O (1,5 %), S (1,2 %) (Table 1). The product obtained after the thermal firing of shungite (shungizit) at +1300 ^{o}C contains in small amounts V (0,015 %), B (0,004 %), Ni (0,0085 %), Mo (0,0031 %), Cu (0,0037 %), Zn (0,0067 %), Co (0,00014 %) As (0,00035 %), Cr (0,72 %), Zn (0,0076 %) and other elements.

Table 1: The chemical composition of shungites from Zazhoginsky deposit (Karelia, Russian Federation), in % (w/w)

№	Chemical component	Content, % (w/w)
1	C	30,0
2	SiO_2	57,0
3	TiO_2	0,2
4	Al_2O_3	4,0
5	FeO	0,6
6	Fe_2O_3	1,49
7	MgO	1,2
8	MnO	0,15
9	CaO	0,3
10	Na_2O	0,2
11	K_2O	1,5
12	S	1,2
13	H_2O	1,7

In comparison with shungite, zeolite comprises a microporous crystalline aluminosilicate mineral commonly used as a commercial adsorbent, three-dimensional framework of which is formed by linking via the vertices the tetrahedra $[AlO_4]^{2-}$ and $[SiO_4]^{2-}$ [3]. Each tetrahedron $[AlO_4]^{2-}$ creates a negative charge of the carcasses compensated by cations (H^+, Na^+, K^+, Ca^{2+}, NH_4^+, etc.), in most cases, capable of cation exchange in solutions. Tetrahedrons formed the secondary structural units, such as six-membered rings, five-membered rings, truncated octahedra, etc. As a result the zeolite framework comprises interacting channels and cavities forming a porous structure with a pore size of 0,3–1,0 nm. Average crystal size of the zeolite may range from 0,5 to 30 μm.

The empirical formula of zeolite can be represented as follows:

$$M_{2/n}O \cdot Al_2O_3 \cdot \gamma SiO_2 \cdot wH_2O,$$

where n – the cationic charge (n = 1–2), γ – the molar ratio of oxides of silicon and aluminum in the zeolite framework, indicating the amount of cation exchange positions in the structure (y = 2–∞), w – the amount of water.

The composition of zeolite is analogous to that of shungite (Table 3), except for carbon which does not occur in zeolite. The amounts of core elements (SiO_2, TiO_2, Al_2O_3, FeO, Fe_2O_3, MgO, CaO, Na_2O, K_2O, S) constituting this mineral differ from that of shungite: their content is higher than that of shungite, except for TiO_2 and K_2O, the contents of which in zeolite were dicreased (Table 2). The content of microelements as V (0,0272 %), Co (0,0045 %), Cu (0,0151 %), Mo (0,0012 %), As (0,0025 %), Ni (0,0079 %), Zn (0,1007 %), Zn (0,1007 %) was somewhat increased in zeolite, while the content of Ba (0,0066 %) and Cr (0,0048 %) was increased (Table 2).

Table 2: The chemical composition of zeolite (Bulgaria), in % (w/w)

№	Chemical component	Content, % (w/w)
1	SiO_2	22,14
2	TiO_2	0,01
3	Al_2O_3	17,98
4	FeO	23,72
5	Fe_2O_3	1,49
6	MgO	14,38
7	MnO	0,61
8	CaO	0,36
9	Na_2O	0,5

10	K_2O	0,4
11	S	0,32
12	P_2O_5	0,06
13	Ba	0,0066
14	V	0,0272
15	Co	0,0045
17	Cu	0,0151
18	Mo	0,0012
19	As	0,0025
20	Ni	0,0079
21	Pb	0,0249
22	Sr	0,0021
23	Cr	0,0048
24	Zn	0,1007
25	H_2O	1,43

The physical and chemical properties of shungite have been sufficiently studied recently [4]. The density of shungite makes up 2,1–2,4 g/cm^3; the porosity – up to 5 %; the compressive strength – 1000–1200 kgf/cm^2; the conductivity coefficient – 1500 SI/m; the hermal conductivity coefficient – 3,8 W/m·K, the adsorption capacity – up to 20 m^2/g.

Shungites differ in composition of their mineral matrix (aluminosilicate, siliceous, carbonate), and the amount of carbon in schungite samples. Shungite minerals with silicate mineral basis are divided into low-carbon (5 % C), medium-carbon (5–25 % C), and high-carbon schungites (25–80 % C) [5]. The sum of (C + Si) in shungites of Zazhoginsky deposit (Karelia, Russian Federation) is varried within 83–88 % as shown in Figure 1.

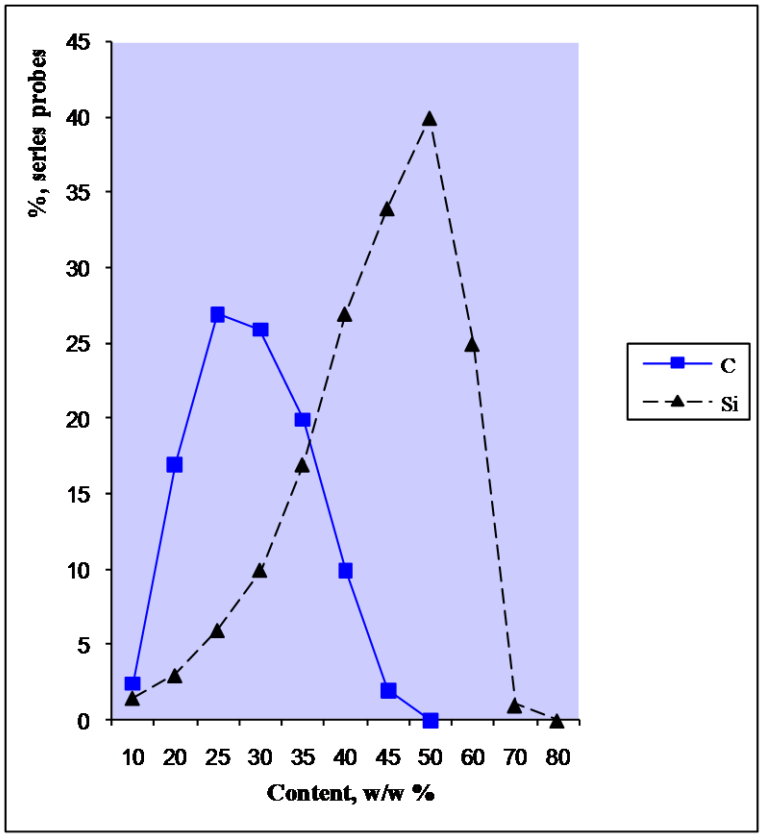

Figure 1. The distribution (%) of carbon (C) (solid line) and silicon (Si) (dotted line) in shungate samples from Zazhoginsky deposit (Karelia, Russian Federation) according to atomic emission spectrometry (AES)

The crystals of the crushed, fine ground shungite possess strong bipolar properties. This results in a high adhesion, and the ability of shungite to being mixed with almost all organic and inorganic substances. Besides, shungite has a broad spectrum of bacterecidal properties; the mineral is the actively adsorptive against some bacterial cells, phages, and pathogenic saprophytes [6].

The unique properties of the mineral are defined by the structure and composition of its constituent elements. Schungite carbon is equally distributed in the silicate framework of fine dispersed quartz crystals having the size of 1–10 μm [7, 8], as confirmed by studying of ultra-thin sections of shungite by transmission electron microscopy (TEM) in absorbed and backscattered electrons.

The carbonaceous material of shungite is the product of a high degree of carbonization of hydrocarbons. Its elemental composition (%, w/w): C – 98,6–99,6; H – 0,15–0,5; (H + O) – 0,15–0,9 [9]. With virtually constant elemental composition of shungite, the carbonaceous matter is demonstrated the variability in its structure – both molecular and supramolecular, as well as surface, and porous structure. X-ray studies showed that the molecular structure of schungite carbon is represented by a solid uncristallized carbon, which components may have been in a state close as to the graphite and the carbon black and the glassy carbon as well, i.e. the maximally disordered [10]. Carbonaceous matter of shungite having a strongly marked structural anisotropy shows a significant increase in the diamagnetism at low temperatures that is a characteristic feature for fullerites [11].

The basis of the shungite carbon compose the hollow carbon fullerene-like multilayer spherical globules with a diameter of 10–30 nm, comprizing inclusive packages of smoothly curved carbon layers covering the nanopores. The globule structure is stable relative to the shungite carbon phase transitions into other allotropic carbon forms. Fullerene-like globules (the content of fullerenes makes up 0,001 %) may contain from a few dozen to a several hundred carbon atoms and may vary in shape and size [12].

A convenient method to obtain information on the composition and the structure of a mineral is IR spectroscopy. IR spectra can usually be obtained with the amount of 0,5–3,0 mg of the sample, i.e. significantly less than required for NMR. In contrast to the NMR the measuring of IR-spectra is possible for solid compounds, which allows the study even insoluble solid substances.

By the method of IR-spectroscopy in the range of vibrations in the crystal mineral framework it is possible to obtain the information:

a) on the composition of the mineral and its components;

b) on the structure of the framework, particularly the lattice ratio type C/SiO_2 or SiO_2/Al_2O_3;

c) on the nature of the surface of the structural groups, which often serve as adsorption and catalytically active sites.

The wave absorption in the infrared region (400–4000 nm) is caused by the vibrational motion of the molecules associated with changes in bond lengths (stretching vibrations, v) or bond angles between the atoms (deformation vibrations, δ). IR spectrum of the carbon containing organic compound ranges from 400–4000 cm^{-1} and allows identify these compounds. However, often the interpretation of natural carbon-containing minerals is difficult due to their multi-component composition and as the result numerous oscillations in samples. Furthermore, the number of absorption bands in the IR spectra may differ from the number of normal molecular vibrations due to the occurrence of additional bands: overtones, component frequencies, and overlapping lines due to the Fermi resonance.

Studying of shungite by the method of IR-spectroscopy revealed the presence at least seven main maxima in the IR-spectrum of shungite, detected at 2,90; 3,18; 3,32; 6,13; 7,14; 8,59; 9,21 μm, or 3448; 3141; 3016; 1630; 1400; 1164 and 1086 cm^{-1} corresponding to oscillations of various organic group types in shungite (Fig. 2).

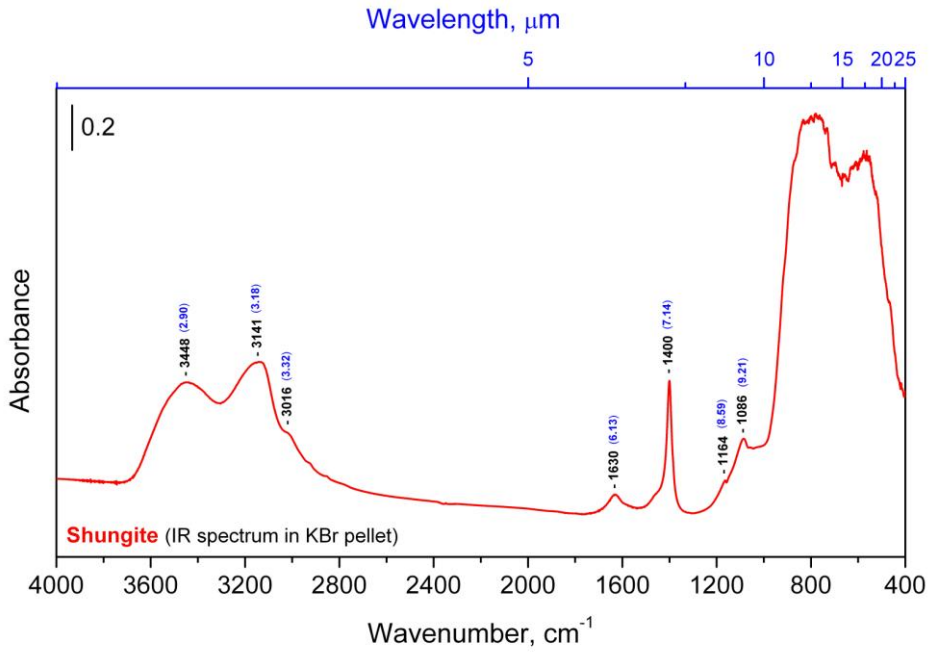

Figure 2. IR-spectra of shungite in KBr pellet (spectral range: average IR – 370–7800 cm^{-1}; visible – 2500–8000 cm^{-1}; the permission – 0,5 cm^{-1}; accuracy of wave number – 0,1 cm^{-1} on 2000 cm^{-1})

The average IR region is the most informative and marked as fundamental. In turn, this area is divided into the "fingerprint" region (700–1500 cm^{-1}) and the region of characteristic bands (1500–4000 cm^{-1}).

When interpreting the IR spectra the most informative are the region at 2500–1500 cm^{-1} and the region at 4000–2500 cm^{-1}. Analysis of the first of these allows determine the presence in the sample the unsaturated compounds: C=C, C≡C, C=O, C=N, C≡N, as well as the aromatic and heteroaromatic nucleus. The absorption bands in the region at 4000–2500 cm^{-1} can identify functional groups as O–H, N–H, S–H, as well as various types of carbon-hydrogen C_{sp3}–H, C_{sp2}–H, C_{sp}–H, (O=) C–H-bonds.

The IR spectra of organic compounds can be divided into three main areas: 1) 4000–2500 cm^{-1} – a region of stretching vibrations of single bonds X–H: O–H, N–H, C–H, S–H; 2) 2500–1500 cm^{-1} – a region of stretching vibrations of multiple bonds X=Y, X≡Y: C=C, C=O, C=N, C≡C, C≡N; 3) 1500–500 cm^{-1} – a region of stretching vibrations of single bonds X–Y: C–C, C–N, C–O and deformation vibrations of single bonds X–H: C–H, O–H, N–H.

Table 3: Characteristic vibrational frequencies of organic compounds [13]

Groups and types of oscillations	The range of frequencies (cm^{-1}), the intensity of the absorption bands
Covalent C–H bond	
Alkanes C_{sp3}–H stretching, v deformational (I) deformational (II)	 2975–2860 (intensive) 1470–1430 (average) 1380–1370 (intensive)
O–CH_3 Stretching	2820–2810 (intensive)
CH_3Hal (F, Cl, Br, I) stretching, v	3058–3005 (intensive)

Alkenes C_{sp2}–H stretching, v (=CH_2) deformational, δ (–CH=CH_2) stretching, v (=CH–) deformational, δ (–CH=CH–) *trans-* *cis-*	 3095–3075 (average) 1420–1410 (intensive) 3040–3010 (average) 1310–1295 (average) 970–960 (intensive) ~690 (average)
Aromatic hydrocarbon $C_{arom.}$–H stretching, v deformational, δ	 ~3030 (intensive) 900–690 (intensive)
Aldehydes stretching, v (I) stretching, v (II)	 2900–2820 (not intensive) 2775–2700 (not intensive)
Alkynes C_{sp}–H stretching, v (≡C–H) deformational, δ (–C≡C–H)	 ~3300 (intensive) 680–610 (intensive)
Covalent bonds X–H	
O–H stretching, v deformational, δ	 3650–3590 (average, narrow) 1450–1250 (average, wide)
H-linked bond stretching, v: alcohols, phenols, carbohydrates, carboxylic acids	 3550–3200 (intensive, wide) 2700–2500 (wide)
N–H Primary amines and amides (–NH–) stretching, v (2 bands) deformational, δ (amid band II)	 3500–3300 (average) 1650–1590 (intensive-average)
Secondary amines and amides (–NH–) stretching, v (I band) deformational, δ (amide band II)	 3500–3300 (average) 1650–1550 (not intensive)
Amino acids stretching, v (NH_3^+) amino acid band I amino acid band II	 1660–1610 (not intensive) 1550–1485 (average)
Imines (+NH–) stretching, v (I band)	 3400–3300 (average)
S–H stretching, v	 2600–2550 (average)
P–H stretching, v	 2440–2350 (average, wide)
Si–H stretching, v	 2280–2080 (average)
Covalent bonds X–Y	
C_{sp3}–C_{sp3} stretching, v	 1250–1200 (intensive)
C–O stretching, v: primary alcohols secondary alcohols tertiary alcohols phenols	 1075–1000 (intensive) 1150–1075 (intensive) 1210–1100 (intensive) 1260–1180 (intensive)

Ethers	
di-alkyl (–CH_2–O–CH_2–)	1150–1060 (very intensive)
aromatic (Ar–O–Ar)	1270–1230 (very intensive)
C–N	
stretching, v:	
aliphatic amines	1220–1020 (average-not intensive)
primary aromatic amines	1340–1250 (intensive)
secondary aromatic amines	1350–1280 (intensive)
tertiary aromatic amines	1360–1310 (intensive)
aliphatic nitro compounds	920–830 (intensive)
aromatic nitro compounds	860–840 (intensive)
C–Hal	
stretching, v:	
C–F	1400–1000 (very intensive)
C–Cl	800–600 (intensive)
C–S	
stretching, v	710–570 (not intensive)
C–P	
stretching, v	800–700 (shifting)
C–O	
stretching, v	870–690 (shifting)
Double covalent bonds X=Y	
C=C	
stretching, v	
isolated double bond (C=C)	
alkenes	1670–1620 (shifting)
cumulated double bonds (C=C=C)	
allenes	~1950 (intensive)
	~1060 (average)
Conjugated double bonds	
(C=C–C=C or C=C–C=O)	
alkadienes and enones	1640–1600 (intensive)
benzene ring (multiple bands)	~1600 (shifting)
	~1580 (shifting)
	~1500 (shifting)
	~1450 (shifting)
C=O	
stretching, v	
saturated aldehydes, ketones, carboxylic acid esters	1750–1700 (intensive)
	1755–1720 (intensive)
a-amino acids (COOH)	1600–1560 (intensive)
amino acids (COO^-)	1705–1660 (intensive)
unsaturated aldehydes and aromatic ketones	1700–1630 (intensive)
amides (amid band I)	
C=N	
stretching, v	1690–1630 (shifting)
C=S	
stretching, v	1200–1050 (intensive)
N=O	
stretching, v	
nitrites (–O–N=O) (2 bands)	1680–1610 (intensive)
nitroso (–C–N=O)	1600–1500 (intensive)
nitrosamines (–N–N=O)	1500–1430 (intensive)
C=S	
stretching, v	1200–1050 (intensive)

In the sub-region (700–1500 cm^{-1}) are located the absorption bands of the skeleton of the organic molecules comprising C–C-bond, C–O, C–N (for this region are not characteristic oscillations belonging to separate bonds). The nature of the IR-spectrum in this frequency range varies significantly with small differences in the spectra of the organic compounds, as each compound has its unique distinctive set of absorption bands. It can be used to discriminate between the molecules having the same functional group.

In the spectral range of 1500–4000 cm^{-1} are located all fluctuations of the basic functional groups. These groups act as if being isolated and independently of the rest of the molecule, as their absorption frequencies little change at transition from one compound to another. The characteristic may be the bands corresponding to both the stretching and bending vibrations.

Absorption in the region at 1400–1300 cm^{-1} and 700 cm^{-1} is due to deformation oscillations of CH_3- and CH_2-groups. Stretching vibrations of the terminal C=C bond correspond to the average intensity of the band at 1640 cm^{-1}.

The position band of CH_2-group at 800–700 cm^{-1} is dependent on the carbon chain length and is used to detect the organic compounds containing the polymethylene chain.

In the region of 3095–3010; 2975; 3040–3010 cm^{-1} are located stretching vibrations of C–H aromatic, heteroaromatic, small cycles, halogenated alkyl groups.

The main range of characteristic bands of organic compounds changes from 3100–3000 cm^{-1} for H–C-; N–H-; O–H-bonds; 3100–2800 cm^{-1} – for C–H; $–CH_3$-bonds; 3040–3010 cm^{-1} – for =CH-bonds; 1750–1700 cm^{-1} – for C=O bonds; 1690-1630 cm^{-1} – for C=N-bonds; 1670–1620 cm^{-1} – for C=C-bonds; 1420–1410 cm^{-1} – for CH_2=CH-bonds; 1310-1295 cm^{-1} – for –CH=CH-bonds; 1250–1200 cm^{-1} – for C_{sp3}–C_{sp3}-bonds; 1260–1000 cm^{-1} for C–O-bonds; 1220–1020 cm^{-1} – for C–N-bonds; 1400–1300 cm^{-1} – for CH_2-bonds; 1640–1600 cm^{-1} – for C=C–C=C or C=C–C=O-bonds; 1060–1950 cm^{-1} for conjugated double C=C=C-bonds (Table 3).

Absorption in the region at 3000–2800 cm^{-1} appears as complex band absorption. The position of bands in this area is preserved in all types of aliphatic hydrocarbons. The intensity of the bands depends on the number of CH_2- and CH_3-groups in the molecule. Accumulation of CH_2-groups increases the intensity of the absorption band of 3000–2800 cm^{-1}, whereas the intensity of the band of the CH_3–group changes little. This property is used for quantitative analysis of hydrocarbons. Thus, the composition of shungite is complex; this mineral contains in its composition many functional groups of organic compounds with different types of bonds, which is due to its complex organic composition.

Evaluation of the mathematical model of interaction of shungite and zeolite with different types of water

Other method for obtaining the information about the average energy of hydrogen bonds in an aqueous sample is measuring the spectrum of the water state. It was established experimentally that at evaporation of water droplet the contact angle θ decreases discretely to zero, whereas the diameter of the droplet changes insignificantly [14]. By measuring this angle within a regular time intervals a functional dependence f(θ) can be determined, which is designated by the spectrum of the water state (SWS) [15–17]. For practical purposes by registering the SWS it is possible to obtain information about the averaged energy of hydrogen bonds in an aqueous sample. For this purpose the model of W. Luck is used, which consider water as an associated liquid, consisted of O–H…O–H groups [18]. The major part of these groups is designated by the energy of hydrogen bonds (-*E*), while the others are free (*E* = 0). The energy distribution function *f(E)* is measured in electron-volts (eV^{-1}) and may be varied under the influence of various external factors on water as temperature and pressure.

For calculation of the function *f(E)* the experimental dependence between the water surface tension measured by the wetting angle (*θ*) and the energy of hydrogen bonds (*E*) in an aqueous sample is used:

$$f(E) = bf(\theta)/[1-(1+bE)^2]^{1/2},$$

where b = 14,33 eV^{-1}; $\theta = arcos(-1-bE)$

The energy of hydrogen bonds (*E*) measured in electron-volts (eV) is designated by the spectrum of energy distribution. This spectrum is characterized by non-equilibrium process of water droplets evaporation, thus the term "non-equilibrium energy spectrum of water" (NES) is applied.

The difference $\Delta f(E) = f$ (samples of water) $- f$ (control sample of water)

– is designated the "differential non-equilibrium energy spectrum of water" (DNES).

DNES is a measure of changes in the structure of water as a result of external factors. The cumulative effect of all other factors is the same for the control sample of water and the water sample, which is under the influence of this impact.

We studied the distribution of local extremums in water solutions of of shungite and zeolite regarding the energies of hydrogen bonds. The average energy ($\Delta E_{H...O}$) of hydrogen H...O-bonds among individual H_2O molecules was calculated for the water solutions of of shungite and zeolite by NES- and DNES-methods. The research with the NES method of water drops, received after their being exposed for 3 days with shungite and zeolite in deionized water, may also give valuable information on the possible number of hydrogen H...O-bonds as a percent (%) of individual H_2O molecules with different values of distribution of energies of hydrogen bonds (Table 4). These distributions are basically connected with the re-structuring of H_2O molecules with the same energies.

Table 4: Characteristics of spectra of water after 3 day infusion with shungite and zeolite, obtained by NES-method

-E(eV) x-axis	Shungite, % [($-E_{value}$)/ ($-E_{total\ value}$)]	Zeolite, % [($-E_{value}$)/ ($-E_{total\ value}$)]	-E(eV) x-axis	Shungite, % [($-E_{value}$)/ ($-E_{value}$)]	Zeolite, % [($-E_{value}$)/ ($-E_{total\ value}$)]
0,0937	2,85	6,3	0,1187	0	12,4
0,0962	8,8	6,3	0,1212	5,9	6,3
0,0987	5,9	0	0,1237	0	0
0,1012	11,8	12,4	0,1262	0	0
0,1037	11,8	6,3	0,1287	0	18,7
0,1062	0	6,3	0,1312	8,8	6,3
0,1087	0	0	0,1337	2,85	0
0,1112	5,9	0	0,1362	0	0
0,1137	11,8	0	0,1387	11,8	2,4
0,1162	11,8	6,3	–	–	–

The distribution [%, ($-E_{value}$)/($-E_{total\ value}$] of water molecules in water solution of shungite/zeolite according to energies of hydrogen bonds and local extremums in NES and DNES spectra of water solutions of of shungite and zeolite is shown in Fig. 3 and Table 5. The average energy ($\Delta E_{H...O}$) of hydrogen H...O-bonds among individual molecules H_2O after the treatment of shungite and zeolite with water was measured to be at -0,1137 eV for shungite and -0,1174 eV for zeolite. The result for the control sample (deionized water) was -0,1162 eV. The results obtained with the NES method were recalculated with the DNES method. Thus, the result for shungite measured with the DNES method was +0,0025±0,0011 eV and -1,2±0,0011 eV for zeolite. This difference may indicate on the different mechanisms of interaction of these minerals with water, but also may has been the result of the different composition and the structure of these two minerals, resulting in different behavior while the interaction with water.

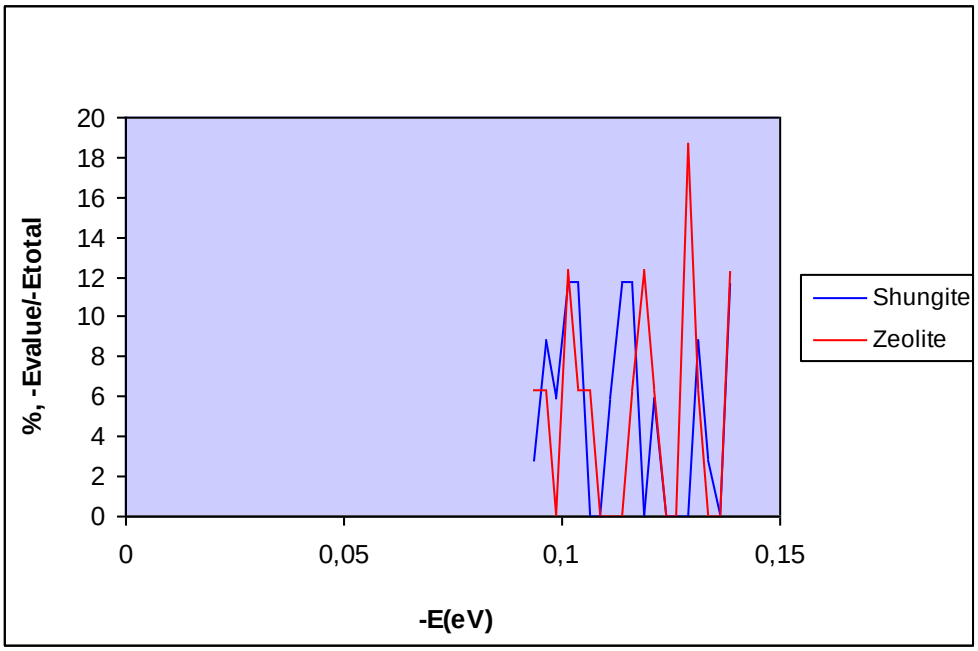

Figure 3. The distribution [%, $(-E_{value})/(-E_{total\ value}$] of water molecules in water solution of shungite/zeolite according to energies of hydrogen bonds ($-E_{value}$) to total result of hydrogen bonds energy

Table 5: Distribution of energies of hydrogen bonds and the local extremums in NES and DNES spectra of water solutions of shungite and zeolite

-E(eV) x-axis	NES Shungite	NES Zeolite y-axis (eV^{-1})	NES Control sample y-axis (eV^{-1})	DNES Shungite y-axis (eV^{-1})	DNES Zeolite y-axis (eV^{-1})	-E(eV) x-axis	NES Shungite y-axis (eV^{-1})	NES Zeolite y-axis (eV^{-1})	NES Control sample y-axis (eV^{-1})	DNES Shungite y-axis (eV^{-1})	DNES Zeolite y-axis (eV^{-1})
0,0937	11,8	25,0	0	11,8	25,0	0,1187	0	50,0	30,8	-30,8	19,8
0,0962	35,3	25,0	30,8	4,5	-5,8	0,1212	23,5	25,0	30,8	7,3	5,8
0,0987	23,5	0	0	23,5	0	0,1237	0	0	0	0	0
0,1012	47,1	50,0	0	47,1	50,0	0,1262	0	0	30,8	-30,8	-30,8
0,1037	47,1	25,0	30,8	16,3	-5,8	0,1287	0	75,0	0	0	75,0
0,1062	0	25,0	0	0	25,0	0,1312	35,3	25,0	0	35,3	25,0
0,1087	0	0	76,9	-76,9	-76,9	0,1337	11,8	0	30,8	-19,0	-30,8
0,1112	23,5	0	15,4	8,1	-15,4	0,1362	0	0	15,0	-15,0	-15,0
0,1137	47,1	0	30,8	16,3	-30,8	0,1387	47,1	50,0	15,0	32,1	35,0
0,1162	47,1	25,0	61,5	-14,4	-36,5	–	–	–	–	–	–

In this regard it should be noted that A. Antonov earlier demonstrated that in the aqueous suspension of tumor cells there was detected a decrease of local maximums; DNES-spectra of aqueous solution containing Ca^{2+} cations have a local minimum of energy at -0,1 eV and a local maximum at -0,11 eV. The interesting fact is that due to the present of calcium in shungite, the aqueous solution of shungite has a local minimum of energy at -0,0987 eV and a local maximum at -0,1137 eV that closely corresponds with the DNES-spectrum of aqueous solution containing Ca^{2+} cations. Thus, by the analyzing the NES- and DNES-spectra of aqueous solutions of shungite and zeolite in water it is possible to evaluate the base of the mathematical model of interaction of these minerals with water, judging by the structural properties, the energies of of hydrogen H…O-bonds and the distribution the individual H_2O molecules in samples with different values of energies.

Table 6 shows the local extremums of different samples of mountain water sources in spectra, as well as ions of Ca^{2+}, Na^{+}, Mg^{2+}, Fe^{2+}, SO_4^{2-} and pH values. For all these types of water is applied a new parameter in Table 6 – the local extremum, measured at -0,1362…-0,1387 eV. Its value in the NES-spectrum is measured as the function of distribution of individual H_2O molecules in water samples according to energy *f(E)* of hydrogen bonds. The function of distribution of individual H_2O molecules according to energy *f(E)* of hydrogen bonds for tap water from Teteven (Bulgaria) is measured up at 23,8±1,2 eV^{-1}.

Table 6: The composition of mountain water sources from Teteven (Bulgaria) and their pH values

Water sources	Ca^{2+}	Na^{+}	Mg^{2+}	Fe^{2+}	SO_4^{2-}	pH	Local extremum* at (-0,1362…-0,1387 eV) (1)	Local extremum* with shungite (-0,1362…-0,1387 eV) (2)	Difference between (2) and (1)
	mg/dm^3 norm (<150)	mg/dm^3 norm (<200)	mg/dm^3 norm (<80)	mg/dm^3 norm (<200)	mg/dm^3 norm (<250)	norm (6,5–9,5)	eV^{-1} norm (>24,1)	eV^{-1} norm (>24,1)	eV^{-1} norm (>24,1)
1. Deionized water (control)	–	–	–	–	–	–	15,4 ±0,8	47,1 ±2,8	31,7 ±1,6
2. Klindiovo	89,9 ±9,0	4,1 ±0,4	6,98 ±0,7	40,2 ±4,0	17,7 ±1,8	8,0 ±0,1	44,4 ±2,2	63,2 ±3,2	18,6 ±0,9
3.Gorna cheshma	103,6 ±10,4	4,2 ±0,4	15,5 ±1,6	9,6 ±0,96	89,9 ±9,0	7,3 ±0,1	51,6 ±2,6	80,0 ±4,0	28,4 ±1,4
4.Dolna cheshma	94,4 ±0,94	2,5 ±0,3	12,10 ±1,21	9,0 ±0,9	15,99 ±1,6	7,9 ±0,1	34,2 ±1,7	51,6 ±2,6	17,4 ±0,9
5. Sonda	113,6 ±11,4	7,3 ±0,7	15,99 ±1,60	5,00 ±0,5	57,2 ±5,7	7,3 ±0,1	54,4 ±2,7	70,6 ±3,5	16,2 ±0,8
6.Ignatov izvor	40,44 ±4,04	0,62 ±0,12	2,46 ±0,25	13,0 ±1,4	17,9 ±1,8	6,82 ±0,1	48,0 ±2,4	85,7 ±4,3	37,7 ±1,9
7. Gechovoto	66,0 ±6,0	1,46 ±0,15	2,1 ±0,2	11,4 ±1,1	15,9 ±1,6	7,94 ±0,1	41,7 ±2,1	84,2 ±4,2	42,5 ±2,1

*Notes: The function of distribution of individual H_2O molecules according to energy *f(E)* of hydrogen bonds for tap water in Teteven (Bulgaria) is 23,8±1,2 eV^{-1}; results refer to the influence of shungite on different sources of mountain water according to energy *f(E)* of hydrogen bonds.

There are obtained new data for the influence of shungite on NES- and DNES-spectra of different mountain water sources and characteristics of spectra (Table 6). The peculiarities consist in the values of the local extremum measured at -0,1362…-0,1387 eV. It was detected the tendency of the increasing of local extremums in aqueous solution of shungite in water regarding the same mountain water samples as regard to the control sample. The dependence of local extremums detected at -0,1362…-0,1387 eV has an inversely character dependent for the ion content in water for difference at -0,1362…-0,1387 eV of the shungite solution in mountain water and the same water as a control sample. These results suggest the restructuring of energy values among individual H_2O molecules with a statistically reliable increase of local maximums in DNES-spectra. The data obtained are very promising and need to be scrutinized seriously. The research will be continued in future with new experiments.

Conclusions

The fullerene-containing natural mineral shungite and microporous crystalline aluminosilicate mineral zeolite have a complex multicomponent composition. The efficiency of using and studying these two natural minerals is stipulated by the high range of valuable properties (absorption, catalytic, antioxidant, regenerative), high environmental safety and relatively low cost of filters based on shungite and zeolite as well as existence of the extensive domestic raw material base of shungite and zeolite deposits. All these factors contribute to the further studies. As the result of our studies the base of the mathematical model describing the interaction of these two minerals with water was established. It allows better understand, how these minerals interact with H_2O molecules in water solutions in order to explain the physical-chemical and adsorption properties of these minerals.

Acknowledgements

The authors wish to sincerely thank Engineer Assen Toshev (Sofia, Bulgaria) for his help in drawing up the diagrams, Maria Marinkova (Batashki Karlak Ltd, Batak, Bulgaria) and Emil Manolov (Scientific Production Enterprise "Bulman–Shungite Ltd." & Veliko Turnovo Ltd.) for close collaboration under the research project for influence of shungite on physical-chemical properties of mountain water.

References:

1. Khavari-Khorasani G. The nature of carbonaceous matter in the Karelian shungite / G. Khavari-Khorasani, D.G. Murchison // *Chem. Geol.* 1979. Vol. 26. P. 165–82.

2. Volkova I.B. Petrology and genesis of the Karelian shungite-high rank coal / I.B. Volkova, M.V. Bogdanov // *Int. J. Coal Geol.* 1986. Vol. 6. P. 369–79.

3. Panayotova M. Kinetics of heavy metal ions removal by use of natural zeolite / M. Panayotova, B. Velikov // *Journal of Environmental Science and Health*. 2002. Vol. 37, № 2. P. 139–147.

4. Parfen'eva L.S. Electrical conductivity of shungite carbon / L.S. Parfen'eva // *Solid State Physics*. 1994. Vol. 36, № 1. P. 234–236.

5. Kasatochkin V.I. Submikroporous structure of shungites / V.I. Kasatochkin, V.M. Elizen, V.M. Melnichenko, I.M. Yurkovsky, V.S. Samoilov // *Solid Fuel Chemistry*. 1978. № 3. P. 17–21.

6. Khadartsev A.A. Shungites in medical technologies / A.A. Khadartsev, I.S. Tuktamyshev // *Vestnik Novih Medicinskih Technologii*. 2002. Vol. 9, № 2. P. 83–86 [in Russian].

7. Kovalevski V.V. Structure of shungite carbon / V.V. Kovalevski // *Natural Graphitization Chemistry*. 1994. Vol. 39. P. 28–32.

8. Mosin O.V. Composition and structural properties of fullerene analogous mineral shungate / O.V. Mosin, I. Ignatov // *Journal of Nano and Microsyctem Technique*. 2013. Vol. 1. P. 32–40 [in Russian].

9. Golubev E.A. Local supramolecular structures shungite carbon / E.A. Golubev // in *Proc. the Int. Symp. "Carbon-formation in geological history"*. – Petrozavodsk: Publishing House of the Karelian Research Center, Russian Academy of Sciences. 2000. P. 106–110 [in Russian].

10. Kovalevski V.V. Comparison of carbon in shungite rocks to other natural carbons: an X-ray and TEM study / V.V. Kovalevski, P.R. Buseckb, J.M. Cowley // *Carbon*. 2001. Vol. 39. P. 243–256.

11. Jushkin N.P. Globular supramolecular structure shungite: data scanning tunneling microscopy / N.P. Jushkin // *Reports. Acad. Science USSR*. 1994. Vol. 337, № 6. P. 800–803 [in Russian].

12. Reznikov V.A. Shungite amorphous carbon – the natural environment of fullerene / V.A. Reznikov, Y.S. Polehovsky // *Technical Physics Letters*. 2000. Vol. 26, № 15. P. 689–693.

13. Vasiliev A.V. *Infrared spectroscopy of organic and natural products: textbook for students* / A.V. Vasiliev, E.V. Grinenko, A.O. Shchukin, T.G. Fedulina. – SPb.: SPbGLTA, 2007, 54 p. [in Russian]

14. Antonov A. *Research of the nonequilibrium processes in the area in allocated systems* / A. Antonov / Diss. thesis doctor of physical sciences. – Sofia: Blagoevgrad. 2005. P. 1–255.

15. Ignatov I. Structural mathematical models describing water clusters / I. Ignatov, O.V. Mosin // *Journal of Mathematical Theory and Modeling*. 2013. Vol. 3, № 11. P. 72–87.

16. Mosin O.V. The structure and composition of natural carbonaceous fullerene containing mineral shungite / O.V. Mosin, I. Ignatov // *International Journal of Advanced Scientific and Technical Research*. 2013. Vol. 6, № 11–12. P. 9–21.

17. Mosin O.V. The Composition and structural properties of fullerene natural mineral shungite / O.V. Mosin, I. Ignatov // *Nanoengineering*. 2012. Vol. 18, № 12. P. 17–24 [in Russian].

18. Luck W. Infared investigation of water structure in desalination membranes / W. Luck, D. Schiöberg, S. Ulrich // *J. Chem. Soc. Faraday Trans*. 1980. Vol. 2, № 76. P. 136–147.

Published in the Russian Federation
European Reviews of Chemical Research
Has been issued since 2014.
ISSN: 2312-7708
E-ISSN: 2413-7243
Vol. 5, Is. 3, pp. 180-188, 2015

DOI: 10.13187/ercr.2015.5.180
www.ejournal14.com

UDC 544; 547

Synthesis and Photosensitization Evaluation of Some Novel Polyheterocyclic Cyanine Dyes

[*] H.A. Shindy
A.K. Khalafalla
M.M. Goma
A.H. Eed

Department of Chemistry, Faculty of Science, Aswan University, Egypt
81528, Aswan
*Corresponding author E-mail: hashindy2@hotmail.com

Abstract

New polyheterocyclic compound, namely 4-methyl-6-oxo-2-phenyl-furo[(3,2-d)pyrazole; (3,2-d) imidazole] was prepared and oriented to synthesis of some novel monomethine cyanine dyes, dimethine cyanine dyes and mono/di- mixed methine cyanine dyes. The electronic visible absorption spectra of all the synthesized cyanine dyes were investigated in 95% ethanol solution to evaluate their photosensitization properties. Structural identification was carried out via the elemental analysis, visible spectra, mass spectrometry, IR and ^{1}H NMR spectroscopic data.

Keywords: cyanine dyes, synthesis, photosensitization, monomethine cyanine dyes, dimethine cyanine dyes, mixed methine cyanine dyes.

Introduction

Cyanine dyes [1–14] are a class of organic heterocyclic dyes, which have long captured the interest of the scientific community. This is because the class of cyanine dyes has proved to be particularly useful in a diverse and a broad area of science, technology and engineering. Their uses and applications includes but not limited to color and non color (black and white) photography, in high energy laser and digital image storage, analytical reagents over a wide range of pH of media, indicators for solvent polarity, in biological and biomedical use as molecular probes and as fluorescent dyes commonly used for DNA visualization assays. In addition, cyanine dyes [15–28] are widely used as optical recording materials, thermal writing display, laser printers, laser filters, absorptivity and antimicrobial efficiency, for probing lipophilic environments, halophobic pockets of enzymes and components of supramolecular structures.

Taking into account and consideration the above significant benefits of cyanine dyes, in this research paper we prepared new photosensitizers cyanine dyes as new synthesis contribution and spectroscopic investigation in this field and may be used and/or applied in any of the wide mentioned application field of cyanine dyes, particularly as photographic sensitizers in photosensitive material industry, as probes for determining solvent polarity in solution chemistry, and/or as indicators in operations of acid/base titrations.

Experimental

1. General:

All the melting points of the prepared compounds are measured using Electrothermal A9100 melting point 15V, 45W apparatus (Electrothermal®, UK), Chemistry department, Faculty of Science (Aswan University, Egypt) and are uncorrected. The elemental analysis was carried out at the Microanalytical Center of Cairo University by an automatic analyzer Vario EL III (Elementar GmbH, Germany). IR-spectra were measured with a FT/IR 4100 (Jasco Analyt. Instr., Japan), Cairo University. ^{1}H NMR spectra were accomplished using Varian Gemini-300 MHz NMR Spectrometer (Gemini BV, Netherlands), Cairo University. Mass Spectroscopy was recorded on Mas 1: GC-2010 Shimadzu Spectrometer (Shimadzu, Japan), Cairo University. Electronic visible absorption spectra were carried out on a Visible Spectrophotometer, Spectro 24 RS (Labomed Inc, USA), Chemistry department, Faculty of Science (Aswan University).

2. Synthesis:

2.1. Synthesis of 4-methyl-6-oxo-2-phenyl-furo [(3,2-d) pyrazole, (3,2-d) imidazole] (3).

A mixture of equimolar ratios (0.01 mol) of hydantoin (imidazoliol-2,4-dione) (1) and 4-bromo-3-methyl-1-phenyl-5-pyrazolone (2) was dissolved in ethanol (30 ml) containing pyridine (10-20 ml). The reaction mixture was heated under reflux for 6–8 hrs and changed its colour from reddish to deep brown at the end of refluxing. It was filtered while hot to remove any impurities and precipitated by ice water mixture. The product were collected, dried and crystallized from ethanol. The results are listed in Table (1).

2.2. Synthesis of 1-methyl-2-phenyl-furo [(3,2-d) pyrazole, (3,2-d) imidazole]-6[2(4)]-monomethine cyanine dyes (4a–c).

Equimolar ratios (0.01 mol) of compound (3) and ethyl iodide quaternary salts of α-picoline, quinaldine γ-picoline were dissolved in ethanol (30 ml) containing few mls of piperidine (1–2 ml). The reaction mixture was heated under reflux for 3–5 hrs and attained colours from brown to violet at the end of refluxing. The reaction mixtures were filtered on hot to remove unreacted materials, cooled and poured in ice water mixture. The precipitated products were filtered, washed with water, dried, collected and crystallized from ethanol. The data are shown in Table (2).

2.3. Synthesis of 4-formyl-6-oxo-2-phenyl-furo [(3,2-d) pyrazole, (3,2-d) imidazole] (5).

A pure crystallized sample of (3) (0.01 mol) and selenium dioxide were heated under reflux in equimolar ratios (0.01 mol), in dioxane (30 ml) for 16–18 hrs. The reaction mixtures were filtered on hot to remove selenium metal and the filtrate was cooled and precipitated by ice water mixture. The precipitated products were filtered, dried, collected, and crystallized from ethanol to give the 4-carbaldehyde compound (5). The data are given in Table (2).

2.4. Synthesis of 6-oxo-2-phenyl-furo [(3,2-d) pyrazole, (3,2-d) imidazole]-4[2(4)]-dimethine cyanine dyes (6a–c).

A mixture of equimolar ratios (0.01 mol of compound (5) and N-iodoethane quaternary salts of α-picoline quinaldine γ-picoline were heated under refluxed in ethanol (30 ml) containing few mls of piperidine (1–2 mls) for 3–5 hrs. The reaction mixtures, which attained colours from deep brown to deep violet at the end of refluxing, was filtered. While hot to remove any impurities, cooled and precipitated by ice water mixture. The precipitated products were filtered, washed with water several times, dried, collected and crystallized from ethanol. The data are registered in Table (2).

2.5. Synthesis of 2-phenyl-furo [(3,2-d) pyrazole, (3,2-d) imidazole]-4[2(4)]di-6[2(4)]mono- mixed methine cyanine dyes (7a–c).

To different routes are employed to prepare these cyanine dyes:

Route 1: Piperidine (1–2 mls) was added to an ethanolic solution (30 ml) of (5) (0.01 mol) and bimolar ratio of 1-ethyl (α-picolinium, quinaldinium, γ-picolinium) iodide salts (0.02 mol). These mixtures were heated under reflux for 8 hrs and changed its colours from brown to deep violet colours at the end of refluxing. It was filtered off while hot, concentrated to half its volume, cooled and poured in ice water mixture. The precipitated dyes were filtered, washed with water, and crystallized from ethanol. The data are summarized in Table (2).

Route 2: Equimolar ratios (0.01 mol) of the dimethine cyanine dyes (6a–c) and iodoethane quaternary salts of α-picoline, quinaldine and/or γ-picoline were dissolved in ethanol (20 ml), to which piperidine (1–2 mls) was added. The reaction mixture was refluxed for 6 hrs exhibiting permanent intense violet colour at the end of refluxing. It was filtered while hot, concentrated, cooled and precipitated by adding cold water and ice mixture. The precipitates were collected dried and crystallized from ethanol to give the same dyes obtained by the route (1) characterized by melting points, mixed melting points, same IR and ^{1}H NMR spectral data, Table (2).

3. Photosensitization evaluation:

The electronic visible absorption spectra of the prepared cyanine dyes were examined in 95% ethanol solution and recorded using 1 cm Q_z cell on Visible Spectrophotometer, Spectro 24 RS (Labomed Inc., USA). A stock solution ($1{\cdot}10^{-3}$ *M*) of the dyes was prepared and diluted to a suitable volume in order to obtain the desired lower concentrations. The spectra were recorded immediately to eliminate as much as possible the effect of time.

Results and discussion

1. Synthesis:

An equimolar ratios of hydantoin (imidazoliol-2,4-dione) (1) and 4-bromo-3-methyl-1-phenyl pyrazole-5-one (2) were reacted in ethanol containing pyridine and achieved 4-methyl-6-oxo-2-phenyl-furo[(3,2-d) pyrazole; (3,2-d) imidazole] (3) as new polyheterocyclic starting material compound, Scheme (1), Table (1).

Reaction of (3) and iodoethane quaternary salts of α-picoline, quinaldine and/or γ-picoline in equimolar ratios in ethanol as organic solvent and piperidine as a basic catalyst gives the 6[2(4)]monomethine cyanine dyes (4a–c), Scheme (1), Table (1).

Selenium dioxide oxidation of (3) in dioxane as solvent resulted the 4-carbaldehyde compound (5), Scheme (1), Table (2). Subsequent reaction of (5) and 1-ethyl (α-picolinium, quinaldinium and/or γ-picolinium) iodide quaternary salts in equimolar ratios, in ethanol catalyzed by piperidine produced the 4[2(4)]-dimethine cyanine dyes (6a–c), Scheme (1), Table (2).

Reaction of 1:2 molar ratios of (5) and 2(4)-methyl quaternary salts of α-picoline, quinaldine and/or γ-picoline in ethanol containing few mls of piperidine achieved the 6[2(4)]*mono*-4[2(4)]*di*-mixed methine cyanine dyes (7a–c), Route (1), Scheme (1), Table (2).

Chemical confirmation takes place for the mixed methine cyanine dyes (7a–c) via the route (2) by reactions of the previously prepared dimethine cyanine dyes (6a–c) with iodoethene quaternary salts of α-picoline, quinaldine and/or γ-picoline in equimolar ratios in ethanol as organic solvent and piperidine as a basic catalyst to give the same mixed methine cyanine dyes (7a–c), prepared by the route (1), characterized by the melting point, mixed melting points, same IR and ^{1}H NMR spectral data, Scheme (1) Route (2), Table (2).

The structure of the prepared compounds was confirmed by elemental analysis, Tables (1) and (2), visible spectra, Tables (1) and (2), mass spectrometry, Table (3), IR [29] and ^{1}H NMR [30] spectroscopic data, Table (3).

2. Photosensitization evaluation:

Photosensitization evaluation of the prepared cyanine dyes was carried out via measuring their electronic visible absorption spectra in 95% ethanol solution. The dyes are thought to be better photosensitizers when they absorb light at longer wavelength bands (bathochromic shifted and/or red shifted bands). Consequently the photosensetization of the dyes decreases when they absorb light at shorter wavelength bands (hypsochromic shifted and/or blue shifted bands).

The electronic visible absorption spectra of the monomethine cyanine dyes (dimethine cyanine dyes) 4a–c (6a–c) in 95% ethanol solution represented bands in the visible range of 400–514 nm (405–520 nm). The positions of these bands underwent displacements to give bathochromic and/or hypsochromic shifted bands depending upon the nature of the heterocyclic quaternary salts (A) and their linkage positions. So, substituting (A) = 1-ethyl pyridinium-2-yl salt in the dyes 4a (6a) by A = 1-ethyl quinolinium-2-yl salt to get dyes 4b (6b) causes the bathochromic shift band by 27 nm (30 nm) for the maximum absorption spectra band accompanied by increasing intensity of the absorption bands, Scheme (1), Table (1). This can be attributed to increasing π-delocalization conjugation in the latter dyes 4b (6b) due to the presence of quinoline ring system in comparison to pyridine ring system in the former dyes 4a (6a).

Changing the linkage positions from 2-yl salt residue to 4-yl salt residue moving from dyes 4a (6a) to dyes 4c (6c) resulted in a red shift by 4 nm (4 nm) for the maximum absorption spectra band accompanied by increasing the intensity of the absorption band, Scheme (1), Table (1). This can be related to increasing the length of π-delocalization conjugation to the quaternary nitrogen of the pyridine salt in the γ-picoline dyes 4c (6c) compared to the α-picoline dyes 4a (6a).

Additionally, the electronic visible absorption spectra of the mono/di- mixed methine cyanine dyes (7a–c) in 95% ethanol solution resulted in bands in the visible region 410–530 nm. The position of these bands and their nuclear extinction coefficients is largely effected by the type of the heterocyclic quaternary salts (A) and their linkage positions, Scheme (1), Table (2). This can be attributed to the same reasons cited before in case of the electronic absorption spectra of the monomethine cyanine dyes (3a–c) and the dimethine cyanine dyes (6a–c).

The comparison the electronic visible absorption spectra of the monomethine cyanine dyes (4a–c) with those of the dimethine cyanine dyes (6a–c) reveals that the latter dyes have bathochromic shifted bands than the former dyes. This can be related to increasing the number of methine groups between the basic center (nitrogen atom) and the acidic center (quaternary salt) in latter dyes, Scheme (1), Tables (1) and (2).

Comparing the electronic visible absorption spectra of the mono/di- mixed methine cyanine dyes (7a–c) with those of the monomethine cyanine dyes (4a–c) and/or the dimethine cyanine dyes (6a–c) showed that the former mono/di- mixed methine dyes (7a–c) have red shifted and intensified absorption bands in comparison to the latter monomethine (4a–c) and dimethine (6a–c) cyanine dyes, Scheme (1), Tables (1), (2). This can be attributed to two factors. The first factor is related to increased number of methine units in the former mixed methine cyanine dyes (7a–c) in comparison to the latter monomethine cyanine dyes (4a–c) and the dimethine cyanine dyes (6a–c). The second factor is related to the presence of two electronic charge transfer pathways inside the mixed methine cyanine dyes molecules (7a–c) in correspondence to one electronic charge transfer pathways inside the molecules of the monomethine cyanine dyes (4a–c) and the dimethine cyanine dyes (6a–c), Scheme (2).

Conclusion

From the above discussed results we could conclude that:

1. The electronic visible absorption spectra of the synthesized cyanine dyes in 95% ethanol solution underwent displacements to give bathochromic and/or hypsochromic shifted bands depending upon the following factors:

A) Types of the heterocyclic quaternary salts residue in the dyes molecules in the order of: quinaldine dyes > α-picoline dyes.

B) Linkage positions of the heterocyclic quaternary salts residue in the order of: γ-picoline dyes > α-picoline dyes.

C) Number of the methine units and/or groups in the dyes molecules in the order of: mono/di- mixed methine cyanine dyes > dimethine cyanine dyes > monomethine cyanine dyes.

D) Increasing number of the electronic charge transfer pathways inside the dyes molecule in the order of: two electronic charge transfer pathways dyes > one electronic charge transfer pathways dyes.

2. The intensity of the colours of the monomethine cyanine dyes (4a–c), the dimethine cyanine dyes (6a–c) and the mixed methine cyanine dyes (7a–c) can be attributed to two suggested mesomeric structures (A) and (B) producing a delocalized positive charge over the conjugated system, Scheme (2).

Acknowledgements

We are thankful to the Chemistry department, Faculty of Science, Aswan University, Aswan, Egypt for supporting this work.

References

1. Holt J. S. *J. Mol. Struct*. 2010, 965, 31.

2. Yadav H. O. *Thin Solid Films* 2005, 77, 222.

3. Vannikov A. V., Tameev A. R., Koziov A. A. *Int. Conf. Digital Print Technol.* 2000,156.

4. Kabatc J., Bajorek A., Dobosz R. *J. Mol. Struct*. 2011, 985. 95.

5. Anaya C., Church N., Lewis J. P. *Proteomics* 2007, 7, 215; Karp, N. A., Lilley, K. S. *Proteomics* 2005, 5, 3105.

6. Fegan A., Shirude P. S., Balasubramanian S. *Chem. Commun*. 2008, 2004; Toutchkine A., Nguyen D. V., Hahn K. M. *Bioconjugate Chem*. 2007, 18, 1344.

7. Wang M., Gao M., Miller K. D., Sledge G. W., Hutchins G. D., Zheng Q. H. *Eur. J. Med. Chem.,* 2009, 44, 2300.

8. S. Parvathy, P.T. Liji, A. Kalaiyarasi and R.R. Venkatraman, Synthesis of characterization of heterocyclic cyanine dyes, *Der Chemica Simica*, 2015, 6(1), 42–45.

9. D.P. Ferreira, D.S. Conceicao, Y. Prostota, P.F. Santos, L.F.V. Ferreira, Fluorescene "rhodamine-like" hemicyanines derived from the 6-(N-N-diethylamino)-1,2,3,4-tetrahydroxanthylium system, *Dyes and Pigments*, 2015, 112, 73–80.

10. Christopher D. Gabbutt, Lucy V. Gibbons, B. Mark Heron, Suresh B. Kolla, The intramolecular capture of thermally generated merocyanine dyes derived from naphthopyrans, *Dyes and Pigments*, Vol. 92, Issue 3, March 2012, pp. 995–1004.

11. Zhiyong Li, Shiguo Sun, Fengyu Liu, Yi Pang, Jiangli Fan, Fengling Song and Xiaojun Pang, Large fluorescence enhancement of a hemicyanine by supramolecular interaction with cucurbit[6]uril and its application as resettable logic gates, *Dyes and Pigments*, Vol. 93, Issue 1–3, April–June, 2012, pp. 1401–1407.

12. O. P. Klochko, I. A. Fedyunyayeva, S. U. Khabuseva, O. M. Semenova, E. A. Terpetschnig, L. D. Patsenker, Dyes and Pigments, 2010, 85, 7–15.

13. Ye. M. Poronikb, Yu. P. Kovtunb, S. V. Vasyluka, O. O. Viniychukb, V. M. Yashchuka and O. D. Kachkovskyb, *Journal of Molecular Structure*, Vol. 990, Issue 1–3, 29 March, 2011, pp. 6–13.

14. P. G. Pronkin and A. S. Tatikolov, *High Energy Chemistry*, 2011, Vol. 45, No. 2, pp. 140–146.

15. J. Zhao, Y. Lv, H. Ren, W. Sun, Q. Liu, Y. Fu, L. Wang. Synthesis, spectral properties of cyanine dyes cyclodextrin and their application as the supramolecular host with spectroscopic probe. *Dyes and Pigments*, 2013, 96, 180–188.

16. Christopher D. Gabbutt, Lucy V. Gibbons, B. Mark Heron, Suresh B. Kolla, The intramolecular capture of thermally generated merocyanine dyes derived from naphthopyrans; Photochromism of 5-(diarylhydroxymethyl)-2H-naphtho[1,2-b]pyrans. *Dyes and Pigments*, Vol. 92, Issue 3, March 2012, pp. 995–1004.

17. J. Park, D. Kim, K. Lee, Y. Kim. Reactive cyanine fluorescence dyes indicating pH perturbation of biomolecules. *Bull. Korean Chem. Soc.* 2013, 34(1), 1–4.

18. Mishra A., Behera R. K, Behera P. K., Mishra B. K., Behera G. B. *Chem. Rev*. 2000, 100, 1973 and references therein.

19. Dänhe S. Z. *Chemosphere* 1965, 5, 441; Dänhe S., Leupold D. *Ber. Bunsen-Ges.Phys. Chem*. 1966, 70, 618; Dänhe S., Moldenhauer F. *Prog. Phys. Org. Chem*. 1985, 15, 1; Dänhe S. *Chimia* 1991, 45, 288; Bach G., Dänhe S. Cyanine Dyes and Related Compounds. In: *Rodd's Chemistry of Carbon* Compounds *Supplement, Sainsbury* M., Ed. – Amsterdam: Elsevier Science, 1997; Vol. IVB, Chapter 15, p. 383.

20. Holt J. S. *J. Mol. Struct*. 2010, 965, 31.

21. Schouwink P., von Berlepsch H., Dänhe L., Mahrt R.F. *J. lumin*. 2001, 95, 821.

22. Yadav H.O. *Thin Solid Films,* 2005, 77, 222.

23. Kabatc J., Bajorek A., Dobosz R. *J. Mol. Struct*. 2011, 985, 95.

24. Chen X., Conti P.S., Moats R.A. *Cancer Res*. 2004, 64, 8009.

25. Lee J.J., Huang W.T., Shao D.Z., Uao J.F., Lin M. T. *J. Pharm. Sci*. 2003, 93, 376.

26. Renard B.L., Aubert Y., Asseline U. *Tetrahedron Lett*. 2009, 50, 1897.

27. Ozhalici-Unal H., Lee Pow C., Marks S.A. et al. *J. Am. Chem. Soc.* 2008, 130, 12620.
28. Wang M., Gao M., Miller K.D., Sledge G.W., Hutchins G.D., Zheng Q.H. *Eur. J. Med. Chem.*, 2009, 44, 2300.
29. Wade Jr., L. G., *Organic. Chemistry*, 4th Edn. – New Jersy: Printice Hall, 1999, p. 500.
30. Wade Jr., L. G., *Organic. Chemistry*, 4th Edn. – New Jersy: Printice Hall, 1999, p. 544.

Table (1): Characterization of the prepared compounds (3), (4a–c)

Comp. No.	Nature of products			Molecular formula (M.Wt.)	Analysis%						Absorption spectra in 95% ethanol	
					Calculated			Found				
	Colour	Yield (%)	M.p. (C°)		C	H	N	C	H	N	λ_{max} (nm)	ε_{max} ($mol^{-1}cm^2$)
3	Brown	75	290	$C_{13}H_{10}N_4O_2$ (254)	61.41	3.93	22.04	61.33	3.87	22.00	----------	----------
4a	Brown	51	155	$C_{21}H_{20}N_5OI$ (485)	51.95	4.12	14.43	51.85	4.10	14.38	400, 487	7000, 5900
4b	Violet	65	160	$C_{25}H_{22}N_5OI$ (535)	56.07	4.11	13.08	56.00	4.01	13.00	417, 514	7300, 8200
4c	Deep brown	54	180	$C_{21}H_{20}N_5OI$ (485)	51.95	4.12	14.43	51.89	4.00	14.32	405, 491	7200, 6200

Table (2): Characterization of the prepared compounds (5), (6a–c) and (7a–c)

Comp. No.	Nature of products			Molecular formula (M.Wt.)	Analysis%						Absorption spectra in 95% ethanol	
					Calculated			Found				
	Colour	Yield (%)	M.p. (C°)		C	H	N	C	H	N	λ_{max} (nm)	ε_{max} ($mol^{-1}cm^2$)
5	Red	65	160	$C_{13}H_8N_4O_3$ (268)	58.20	2.98	20.89	58.16	2.81	20.70	----------	----------
6a	Brown	45	185	$C_{20}H_{18}N_5O_2I$ (499)	50.50	3.60	14.02	50.13	3.53	14.01	405, 490	1100, 7900
6b	Deep violet	63	170	$C_{25}H_{20}N_5O_2I$ (549)	54.64	3.64	12.75	54.30	3.40	12.66	420, 520	1500, 1850
6c	Deep brown	52	190	$C_{21}H_{18}N_5O_2I$ (499)	50.50	3.60	14.02	50.45	3.61	14.00	410, 494	7500, 6200
7a	Brown	61	200	$C_{29}H_{28}N_6OI_2$ (730)	47.67	3.83	11.50	47.50	3.75	11.42	410, 510	7000, 6000
7b	Deep Violet	98	195	$C_{37}H_{32}N_6OI_2$ (830)	53.49	3.85	10.12	53.11	3.20	10.00	430, 530	9000, 2100
7c	Deep Brown	53	188	$C_{29}H_{28}N_6OI_2$ (730)	47.67	3.83	11.50	47.52	3.78	11.40	420, 520	1000, 9000

Table (3): IR and ^{1}H NMR (mass) spectral data of the prepared compounds

Comp. No	IR Spectrum (KBr, cm^{-1})	^{1}H NMR Spectrum (DMSO, δ); & (Mass data)
3	588, 700 (mono substituted phenyl) 1031, 1117, 1168 (C-O-C cyclic) 1407, 1495 (C=N) 1603 (C=C) 1719 (C=O) 3437 (NH)	2.15 (s, 3H, CH_3 of position 4). 7.2 (m, 2H, 2NH) 7.4–7.8 (m, 5H, aromatic) M^+: 254
4b	624, 690 (mono substituted phenyl) 756, 810 (o.disubstituted phenyl) 1158 (C-O-C) cyclic) 1486 (C=N) 1597, 1633 (C=C) 2921, 2854 (quaternary salt) 3432 (NH)	1.4 (b, 3H, CH_3 of N-quinolinium) 2.15 (b, 3H, CH_3 of position 4) 3.5 (b, 2H, CH_2 of N-quinolinium) 7.1 (b, 2H, 2NH) 7.3-8.3(m, 12H, aromatic + heterocyclic + -CH=)
5	649, 691(mono substituted phenyl). 1029, 1055, 1130, 1170 (C-O-C cyclic) 1496, 1562 (C=N) 1597 (C=C) 1722 (C=O) 3230 (NH)	7.1 (b, 2H, 2NH) 7.2-8 (m, 5H, aromatic) 10.6 (s, 1H, CHO) M^+: 268
6b	692, 754 (mono substituted phenyl) 794, 828 (o.disubstituted phenyl) 1040, 1087, 1129, 1158 (C-O-C cyclic) 1415 (C=N) 1596 (C=C) 1715 (C=O) 2921, 2851 (quaternary salt) 3428 (NH)	1.2 (b, 3H, CH_3 of N-quinolinium) 3.3 (b, 2H, CH_2 of N-quinolinium) 6.7 (b, 2H, 2NH) 7.2-8.2 (m, 13H, aromatic + heterocyclic + 2-CH=)

Table (3): Continue

Comp. No	IR Spectrum (KBr, cm^{-1})	^1H NMR Spectrum (DMSO, δ); & (Mass data)
7b	648, 692 (mono substituted phenyl) 753, 800 (o.disubstituted phenyl) 1085, 1154 (C-O-C cyclic) 1495, 1463 (C=N) 1595 (C=C) 2923, 2852 (quaternary salt) 3428 (NH)	1.2 (b, 3H, CH_3 of N-quinolinium of position 4) 1.6 (b, 3H, CH_3 of N-quinolinium of position 6) 2.3 (m, 2H, CH_2 of N-quinolinium of position 6) 3.3 (b, 2H, CH_2 of N-quinolinium of position 4) 6.7 (b, 2H, 2NH) 7.3-8.2 (m, 20H, aromatic + heterocyclic + 3 =CH-)

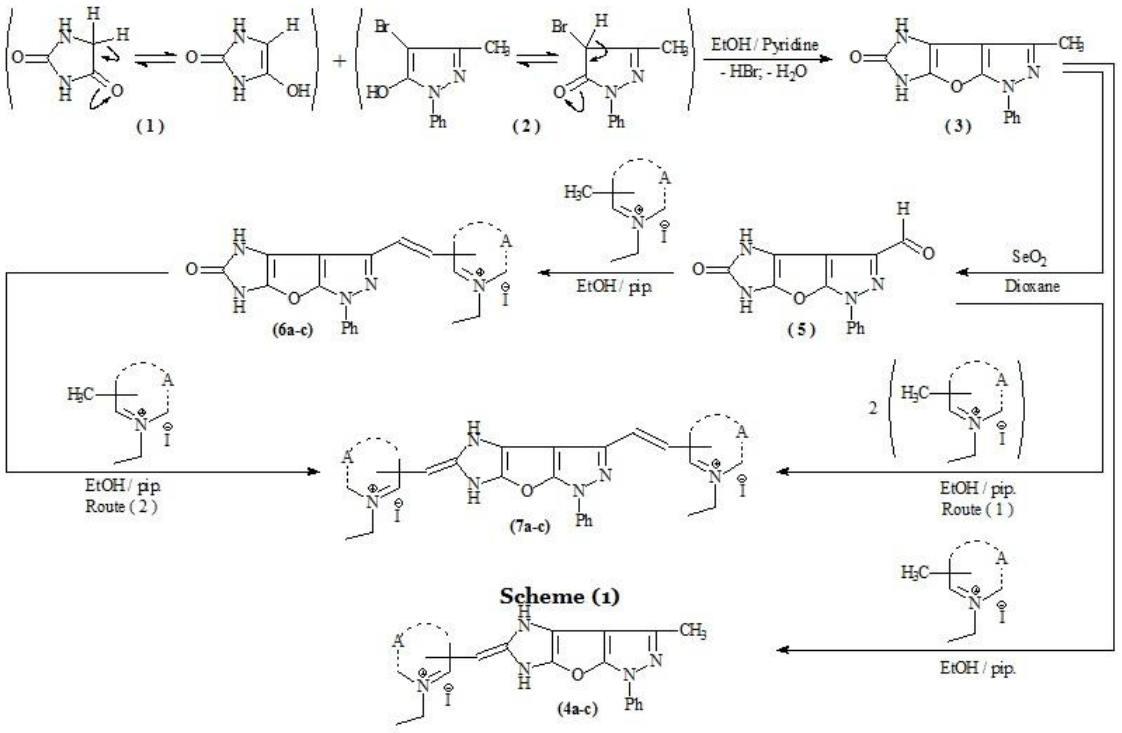

Scheme (1)

Substituents in Scheme (1):
(4a–c); (6a–c); (7a–c): A=1-ethyl=pyridinium-2-yl salt (a); 1-ethyl-quinolinium-2-yl salt (b); 1-ethyl pyridinium-4-yl salt (c).

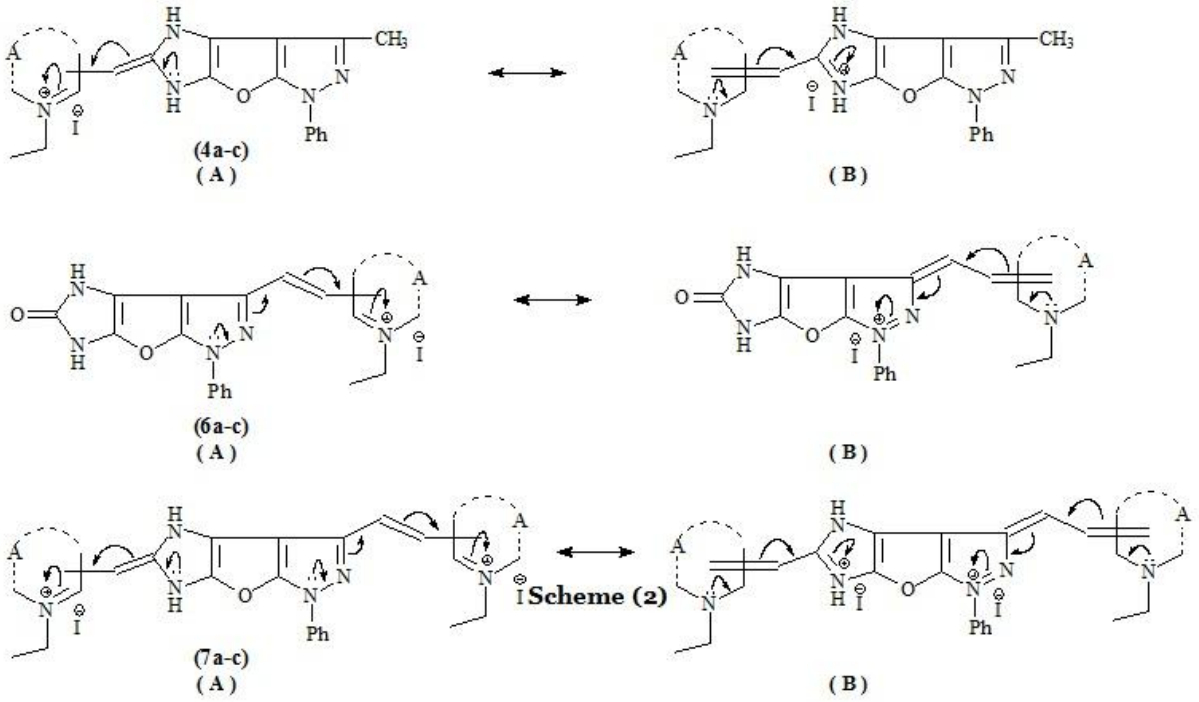

Scheme (2)